AD-A242 363

NAVAL POSTGRADUATE SCHOOL
Monterey, California

THESIS

OPTIMIZATION IN SOLAR HEATING / PHOTOVOLTAIC
SYSTEMS

by

Dimitrios G. Vourazelis

December 1990

Thesis Advisor   Harold A. Titus

Approved for public release; distribution is unlimited

91-14289

91 10 28 087

REPORT DOCUMENTATION PAGE

1a REPORT SECURITY CLASSIFICATION Unclassified		1b RESTRICTIVE MARKINGS
2a SECURITY CLASSIFICATION AUTHORITY		3 DISTRIBUTION / AVAILABILITY OF REPORT
2b DECLASSIFICATION / DOWNGRADING SCHEDULE		Approved for public release; distribution is unlimited.

4 PERFORMING ORGANIZATION REPORT NUMBER(S)	5 MONITORING ORGANIZATION REPORT NUMBER(S)

6a NAME OF PERFORMING ORGANIZATION Naval Postgraduate School	6b OFFICE SYMBOL (If applicable) 33	7a NAME OF MONITORING ORGANIZATION Naval Postgraduate School
6c ADDRESS (City, State, and ZIP Code) Monterey, CA 93943-5000		7b ADDRESS (City, State, and ZIP Code) Monterey, CA 93943-5000

8a NAME OF FUNDING / SPONSORING ORGANIZATION	8b OFFICE SYMBOL (If applicable)	9 PROCUREMENT INSTRUMENT IDENTIFICATION NUMBER

8c ADDRESS (City, State, and ZIP Code)	10 SOURCE OF FUNDING NUMBERS			
	PROGRAM ELEMENT NO	PROJECT NO	TASK NO	WORK UNIT ACCESSION NO

11 TITLE (Include Security Classification)

Optimization in Solar Heating / Photovoltaic Systems

12 PERSONAL AUTHOR(S)   Dimitrios G. Vourazelis

13a TYPE OF REPORT Master's Thesis	13b TIME COVERED FROM _____ TO _____	14 DATE OF REPORT (Year, Month, Day) December 1990	15 PAGE COUNT 65

16 SUPPLEMENTARY NOTATION   The views expressed in this thesis are those of the author and do not reflect the official policy or position of the Department of Defence of the U.S. Government.

17	COSATI CODES		18 SUBJECT TERMS (Continue on reverse if necessary and identify by block number)
FIELD	GROUP	SUB-GROUP	Optimization, solar heating, photovoltaics.

19 ABSTRACT (Continue on reverse if necessary and identify by block number)

This thesis is a design of an alternative system which may provide heating to the Naval Postgraduate School swimming pool. Particularly, it is a solar heating / photovoltaic system designed for a better efficiency and less cost of installation and maintenance. Principles of heat transfer, control and fluid dynamics theory are used for the determination of this heating system elements. The feasibility of its installation and use is analyzed.

20 DISTRIBUTION / AVAILABILITY OF ABSTRACT ☐ UNCLASSIFIED/UNLIMITED ☐ SAME AS RPT ☐ DTIC USERS	21 ABSTRACT SECURITY CLASSIFICATION Unclassified
22a NAME OF RESPONSIBLE INDIVIDUAL Harold A. Titus	22b TELEPHONE (Include Area Code) (408) 646-2560 22c OFFICE SYMBOL EC/Ts

DD Form 1473, JUN 86   Previous editions are obsolete   SECURITY CLASSIFICATION OF THIS PAGE

S/N 0102-LF-014-6603

Optimization in Solar Heating / Photovoltaic Systems.

by

Dimitrios G. Vourazelis
Lieutenant J.G., Hellenic Navy
B.S., Hellenic Naval Academy, 1982

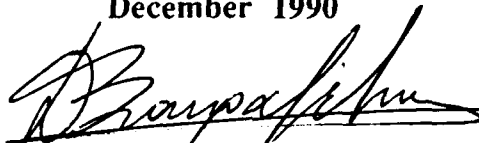Submitted in partial fulfillment of the requirements for the
degree of

MASTER OF SCIENCE IN ELECTRICAL ENGINEERING

from the

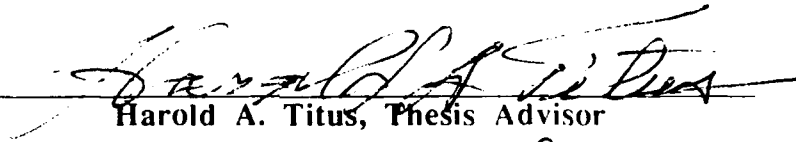NAVAL POSTGRADUATE SCHOOL

December 1990

Author: _____
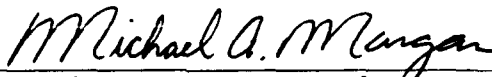Dimitrios G. Vourazelis

Approved by: _____
Harold A. Titus, Thesis Advisor

_____
Sherif Michael, Second Reader

_____
Michael A. Morgan, Chairman
Department of Electrical and Computer Engineering

ABSTRACT

This thesis is a design of an alternative system which may provide heating to the Naval Postgraduate School swimming pool. Particularly, it is a solar heating / photovoltaic system designed for a better efficiency and less cost of installation and maintenance. Principles of heat transfer, control and fluid dynamics theory are used for the determination of this heating system elements. The feasibility of its installation and use is analyzed.

A-\

iii

TABLE OF CONTENTS

LIST OF TABLES

LIST OF FIGURES

I. INTRODUCTION

A. GENERAL

Nowadays, high energy consumption based on fuel has been associated with economic development and a high quality of life. With time, energy users' demand increases, while the fuel reserves are dwindling. The conflict between demand and supply causes an escalation of the fuel cost, which should mandate the research, development and use of alternative resources of energy. We should develop alternative means of energy and fuel conservation.

B. OBJECTIVES

As an example of a heating usage needing optimization, we will analyze and design a new heating system for the swimming pool of the Naval Postgraduate School.

C. SYSTEM DESCRIPTION

The existing system, using fuel to heat the water and electric power to drive the pump for circulation through the heat exchanger and the filters, is old, wastes fuel and is inefficient. Presently, the boiler plant is used to keep the pool at the desired temperature. New solar system designs here offer several alternative energy schemes with various tradeoffs. An optimum design is suggested.

The objective is the design and modeling of a system using a minimum area of collectors and electric power to provide a maximum thermal energy to the pool. Taking into account its geometry and masonry materials, as well as accurate weather data of the Monterey area taken from meteorology statistics (Table 1), and applying heat transfer principles, a total heat loss is calculated. That heat loss is balanced by the collectors and the solar irradiation providing thermal energy to the water and maintaining its temperature. The

1

heat loss due to conduction, convection, radiation and evaporation is calculated for each month in Chapter II.

Power vs cost tradeoffs are made for low-power DC pumps with photovoltaic and a separate filter pump system and standard AC.

TABLE 1. WEATHER DATA FOR THE MONTEREY AREA.

MONTH	MONTHLY TEMPERA-TURE (degrees F)			WIND SPEED (mph)	RELATIVE HUMIDITY %
	Average maximum	Average minimum	Mean	Average	Average
January	60.0	43.0	51.5	4 (1989)	72
February	61.8	44.5	53.1	4 (1989)	72
March	61.8	44.6	53.2	4 (1989)	73
April	63.4	45.5	54.4	5 (1989)	75
May	64.4	47.6	56.0	6 (1989)	76
June	67.0	50.1	58.5	6 (1989)	77
July	68.0	51.5	59.7	5 (1989)	79
August	69.0	52.6	60.8	5 (1989)	79
September	72.0	52.8	62.4	4 (1989)	78
October	70.3	50.9	60.6	5 (1989)	76
November	65.4	47.0	56.2	4 (1989)	74
December	61.0	43.7	52.3	4 (1989)	73

II. HEAT TRANSFER ANALYSIS

A. HEAT TRANSFER DUE TO CONDUCTION

It is considered that the heat is transferred by conduction under one-dimensional, steady-state conditions. The *one-dimensional* refers to the fact that one coordinate is needed to describe the spatial variation of the temperature, and the heat transfer occurs in that direction only, as can be seen in Figure 1. The system (ground-walls of the swimming pool water) is characterized by steady conditions, since there is no energy generated per unit volume of the medium of the wall, assuming that the temperature is independent of time. The heat diffusion equation is,

$$\frac{\partial}{\partial x}\left(k\frac{\partial T}{\partial x}\right) + \frac{\partial}{\partial y}\left(k\frac{\partial T}{\partial y}\right) + \frac{\partial}{\partial z}\left(k\frac{\partial T}{\partial z}\right) + \dot{q} = \rho c_p \frac{\partial T}{\partial t} \qquad (2.1)$$

where,

$\dot{q}$ = energy rate, which is generated per unit volume of the medium

$\rho c_p \dfrac{\partial T}{\partial t}$ = time rate of change of the internal (thermal) energy of the medium

per unit volume.

can be expressed as:

$$\frac{d}{dx}\left(k\frac{dT}{dx}\right) = 0 \qquad (2.2)$$

The general solution of the eq.(2.2) is : $T(x) = C_1 x + C_2$, with $T(0) = T_{S,1}$ and $T(L) = T_{S,2}$. Applying these conditions to the equation we have : $C_2 = T_{S,1}$ and at $x = L$, $T_{S,2} = C_1 L + C_2 = C_1 L + T_{S,1}$, that means $C_1 = (T_{S,2} - T_{S,1}) / L$.

3
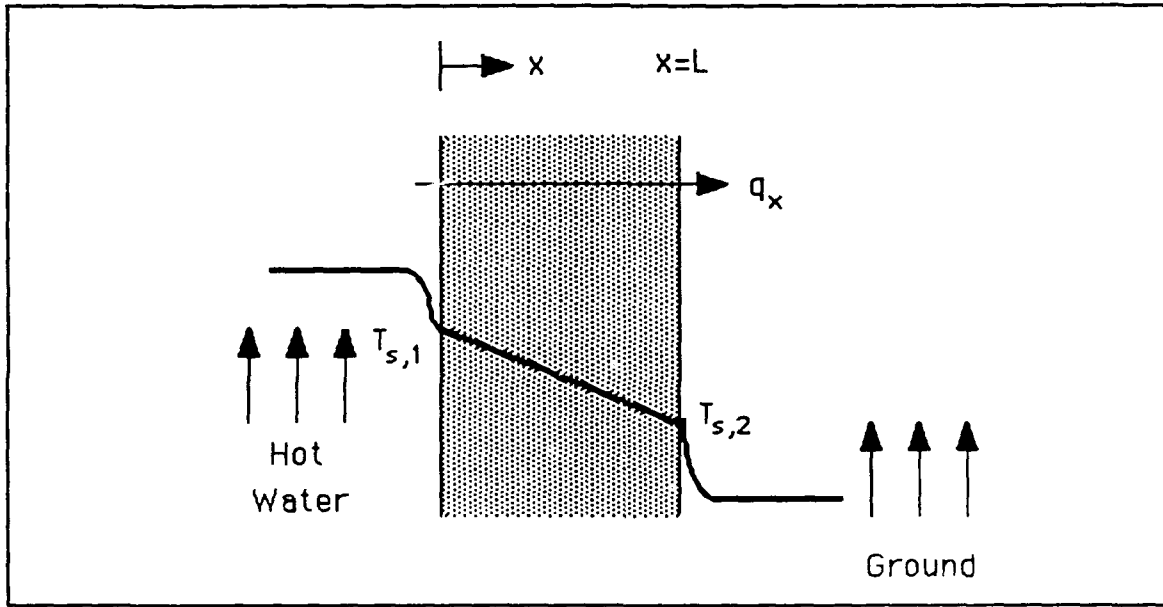
Figure 1. Heat transfer through a plane wall.

Substituting into the general solution, the temperature distribution is then :

$$T(x) = \left(T_{s,2} - T_{s,1} \right) \frac{x}{L} + T_{s,1}$$

It is evident from this result that the temperature varies linearly with x and its rate of change with respect to the x coordinate is:

$$\frac{dT}{dx} = \left(T_{s,2} - T_{s,1} \right) \frac{1}{L} \tag{2.3}$$

Then the conduction heat transfer rate is obtained by using the Fourier's law equation,

$$q_x = - kA \frac{dT}{dx} = - \frac{kA}{L} \left(T_{s,2} - T_{s,1} \right) = \frac{kA}{L} \left(T_{s,1} - T_{s,2} \right) \tag{2.4}$$

4

In our case having a series composite wall (Figure 2), the temperature distribution is the sum of the distributions for each medium separately. Therefore, the temperature distributions for the insulating fiber resin and the concrete block walls are $T_f(x)$ and $T_c(x)$ respectively.

$$T_f(x) = (T_1 - T_p)\frac{x}{L_f} + T_p \tag{2.5}$$

and

$$T_c(x) = (T_g - T_1)\frac{x}{L_c} + T_1 \tag{2.6}$$

where, T_1 is the temperature at the thermal contact between the two walls.

Taking the thermal conductivity coefficients of the fiber resin ($k_i = 0.038$ W/mK) and the concrete block ($k_c = 0.67$ W/mK) from the Tables A-1 and A-2 respectively, the thicknesses of the walls ($L_f = 0.01$m and $L_c = 1.524$m), the temperatures of the water, and the ground (T_p and T_g) and applying into the eq. (2.4), the inlet and outlet transfer rates are obtained.

$$q_{x,\,in} = -\frac{k_f A}{L_f}(T_p - T_1) \tag{2.7}$$

and

$$q_{x,\,out} = -\frac{k_c A}{L_c}(T_1 - T_g) \tag{2.8}$$
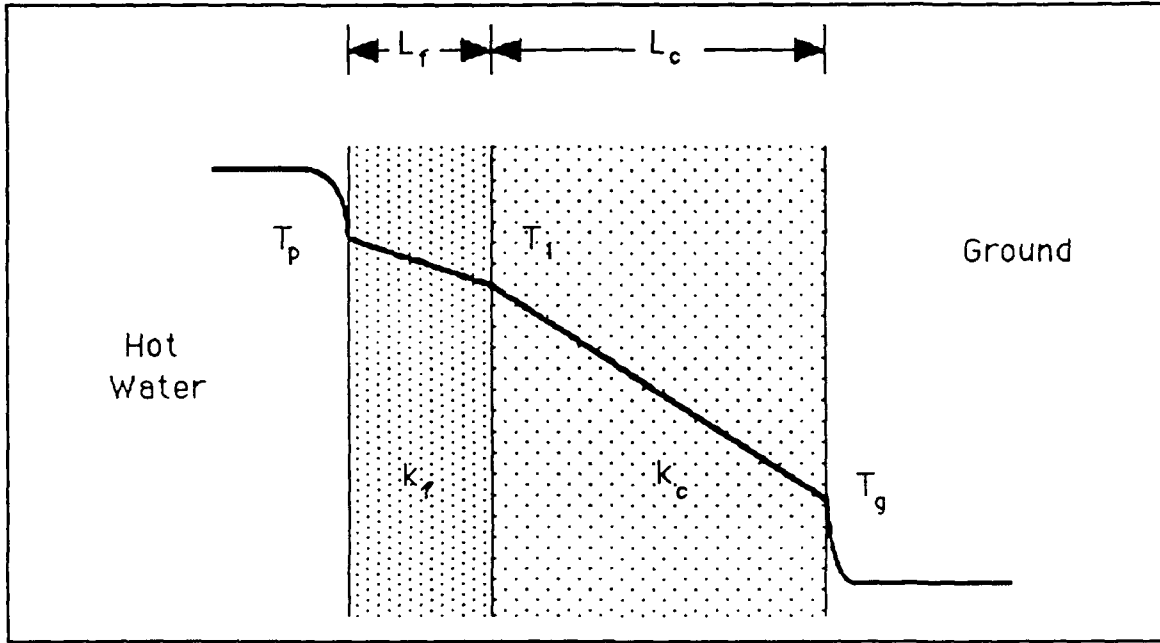
Figure 2. Temperature distribution into the swimming pool walls

The inlet heat rate $q_{x,in}$, which is transferred through the composite wall, *from the hot* water (swimming pool water at 80°F=300°K) towards the *cold* ground, which is assumed to have a temperature 2°K lower than the mean temperature of the air, is equal to the outlet heat rate $q_{x,out}$.

$$q_{x,\,in} = q_{x,\,out} \Leftrightarrow \frac{k_f A}{L_f}(T_p - T_1) = \frac{k_c A}{L_c}(T_1 - T_g) \Leftrightarrow$$

$$\Leftrightarrow \frac{k_f(T_p - T_1)}{L_f} = \frac{k_c(T_1 - T_g)}{L_c} \tag{2.9}$$

Plugging in the values in the above equation we obtain the temperature T_1 and then from the eq. (2.7) or (2.8), the conduction heat transfer rate q_x is calculated for each wall and the bottom. Summing up the heat transfer rates for each particular area A_i, the total heat loss due to conduction is obtained for January (Table 2). Similarly working for the mean temperatures in Table 1, the conduction heat losses for each month are calculated, as shown in Table 3.

TABLE 2. CONDUCTION HEAT LOSS (JANUARY).

	A_1 (45m^2)	A_2 (65m^2)	A_3 (22m^2)	A_4 (65m^2)	A_5 (652m^2)	A_{tot}(849m^2)
q_i (W)	331.05	478.19	161.85	478.19	4796.64	6245.93

Therefore, q_{cond}= 6245.93 Watt = 15.86 MBtu per month (for January).

TABLE 3. MONTHLY CONDUCTION HEAT LOSSES.

MONTH	Watts	MBtu per month
January	6245.93	15.86
February	5780.91	13.26
March	5764.18	14.63
April	5540.04	13.61
May	5242.26	13.31
June	4777.28	11.74
July	4553.14	11.56
August	4349.06	11.04
September	4051.32	9.95
October	4385.86	11.13
November	5205.5	12.79
December	5931.46	15.06

B. HEAT TRANSFER DUE TO CONVECTION

The term convection refers to energy transfer which occurs between a fluid in motion and a bounding surface when these two are in different temperatures. In this study the moving fluid is considered to be the atmospheric wind blowing in average speeds as in Table 1 for each month, and the bounding surface is the surface of the water of the pool. Since we have a flow caused by external means, we speak of forced convection.

Considering a small area A_s of the water surface with temperature T_s, the wind speed V, and air temperature T_∞; a local heat flux q'' occurs which is proportional to the difference $(T_s - T_\infty)$, that is:

$$q'' = h(T_s - T_\infty)$$

where, h=local convection coefficient.

By integrating the local heat flux q'' over the area A_s, the total heat transfer rate q is obtained.

$$q = \int_{A_s} q'' dA_s$$

and

$$q = (T_s - T_\infty) \int_{A_s} h dA_s$$

Then defining the average convection coefficient h' for the entire surface, the total heat transfer rate is expressed as:

$$q = h' A_s (T_s - T_\infty) \tag{2.10}$$

Setting the water surface area $A_s = A = 652\ m^2$, the water temperature $T_s = T_p = 80°F = 300°K$ and the air temperature $T = T_a = 56°F = 286.33°\ K$ (for May) the eq. (2.10) becomes:

$$q = h' A (T_p - T_a) \tag{2.11}$$

9
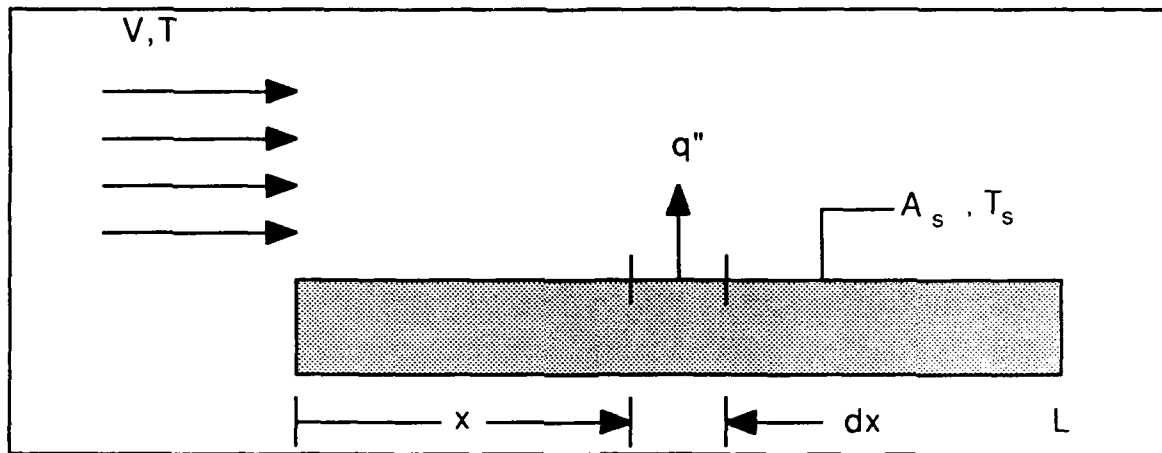
Figure 3. Heat transfer from the surface of the water to the air due to the forced convection.

Assuming that the wind is blowing lengthwise with an average speed as shown in Table 1, we calculate the Reynold's number,

$$R_c = \frac{VL}{v_{air}}$$

where, V is the wind speed, L the length of the swimming pool, and v_{air} the kinematic viscosity of the air. From the Table A-3, for the mean air temperature T_a of each month we get v_{air}, the conductivity coefficient k of the air and the Prandtl number Pr. Thereafter, calculating the Reynold's numbers for each case, we see that the flow over the water surface is turbulent, because $5 \times 10^5 < R_e < 10^8$. Since $0.6 < Pr < 60$ the equation

$$Nu = (0.037 R_e^{4/5} - 871) Pr^{1/3} \qquad (2.12)$$

is used [Ref. 3] for the calculation of the Nusselt number (Nu), which provides a measure of the convection heat transfer occurring at the surface. The Reynold and Prandtl numbers are applied to eq. (2.12) and we get Nu. As described in [Ref. 3:pp.337], the defining expression of Nusselt number is:

$$Nu = \frac{h'L}{k} \qquad (2.13)$$

Solving eq. (2.13) with respect to h' and substituting the obtained values of k, L, and Nu, we get the convection coefficient h'. Finally, the amount of heat transfer due to convection is calculated by applying the values of h', A, T_p, and T_a to the eq. (2.11). Then, we have the results for each month as shown in Table 4.

TABLE 4. MONTHLY CONVECTION HEAT LOSSES.

MONTH	Watts	MBtu per month
January	50816.8	129.01
February	47895.62	109.82
March	47753.03	121.23
April	55404.04	136.11
May	60754.73	154.23
June	54461.63	133.79
July	43915.97	111.49
August	41524.02	105.41
September	31319.06	76.94
October	41944.95	106.48
November	42368.89	104.09
December	49391.38	125.39

C. HEAT LOSS DUE TO THERMAL RADIATION

The heat transfer by thermal radiation is an important process which occurs at a single surface, in this situation, and depends strongly on the surface geometry and orientation, as well as on the water radiative properties and temperature. Thermal radiation is related to energy released as a result of oscillations or transitions of the electrons which constitute the water. These oscillations are sustained by the internal energy, and therefore, the temperature of this matter. The water of the pool, being in a higher temperature T_p than that of the surrounding air, tends to achieve a thermal equilibrium with the atmosphere by

getting cooler. This cooling is associated with a reduction of the internal energy stored by it, and the consequence is the emission of thermal radiation from the surface. This radiation is the energy rate emitted by the water as a result of its temperature T_p and goes on until the matter reaches the atmosphere temperature.

The nature of the thermal radiation is a propagation of electromagnetic waves and more particularly those with a wavelength from approximately 0.1 to 100 μm. This portion of electromagnetic radiation spectrum includes a part of ultra-violet, all of the visible and the infrared. The rate at which the radiation leaves the surface of the water is determined by the equation:

$$q_{rad} = A F \sigma \varepsilon \left(T_p^{\,4} - T_{atm}^{\,4} \right) \qquad (2.14)$$

as in [Ref. 3, pp. 760], where,

A = Area of the surface

F = View factor

σ = Stefan-Boltzmann constant

ε = Emissivity of the water = 0.96 (from Table A-5)

T_p = Water temperature

T_{atm} = Atmosphere temperature = 273°K.

The view factor is a dimensionless number which is defined as the fraction of the radiation leaving the surface of the water and is intercepted by the atmosphere. For this study the view factor is considered F = 1. However, for each month the amount of heat transfer by thermal radiation is the same.

$$q_{rad} = 652m^2 \times 1 \times 5.67 \times 10^{-8} W / m^2 \cdot K^4 \times 0.96 \times \left(300^4 - 273^4\right) = 90336 \text{ Watt}$$

Then the monthly heat loss due to radiation is: q_{rad} = 221.9 MBtu per month.

D. HEAT TRANSFER DUE TO EVAPORATION

The evaporation from a free-water surface is a process associated with water-vapor transfer from the water surface to the air and occurs by the combined processes of convection and diffusion. Figure 4 is the schematic model.

The surface of the pool at temperature T_p is exposed to a stream of moist air. Into the boundary layer, the velocity of the air $V(y)$ varies from zero to V_a at the outer edge. Temperature $T(y)$ decreases from T_p to T_a, and the humidity decreases in the y direction from ϕ_p at the water surface to ϕ_a in the air. The transfer of mass of water-vapor having an internal energy causes a thermal loss whose rate is given by the equation:

$$q_{evap} = h_m h_{fg} (1 - \phi_a) \rho_{a, sat} A \qquad (2.15)$$

where,

h_m = mass transfer coefficient (m/s)

h_{fg} = heat of vaporization

ϕ_a = relative humidity

$\rho_{a,sat}$ = density of the saturated air

A = area of the swimming pool.

14
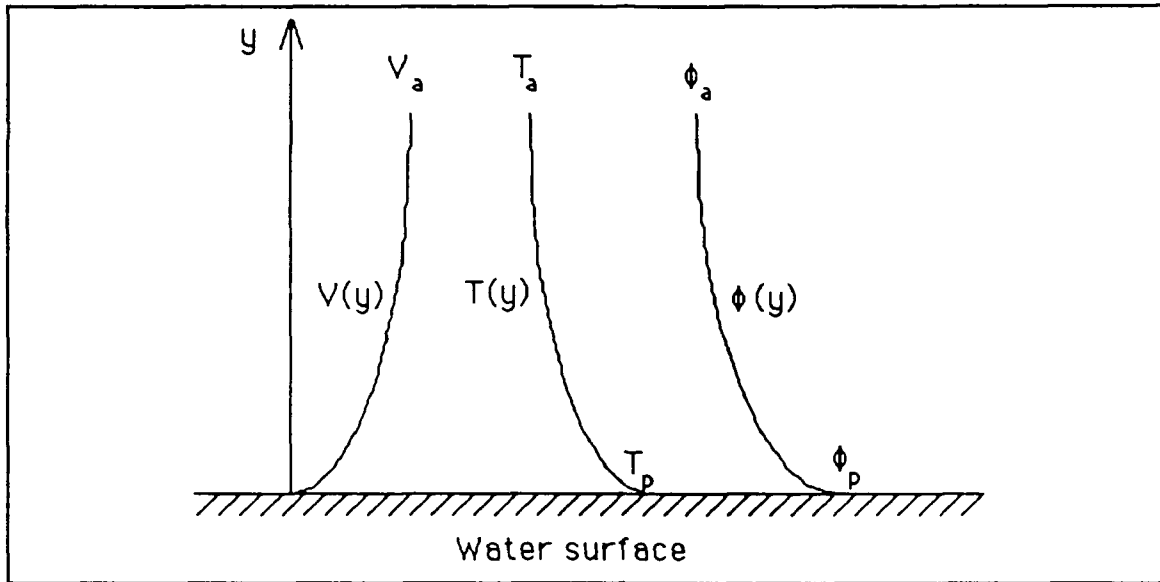
Figure 4. Evaporation of water into moist air.

The mass transfer coefficient is given by the equation:

$$h_m = \frac{h'}{\rho_a c_{p,a} (Sc / Pr)^{2/3}} \qquad (2.16)$$

where,

h' = convection coefficient

ρ_a = air density

$c_{p,a}$ = specific heat of the air

Sc = Schmidt number

Pr = Prandtl number.

15

The values of the above variables in eq. (2.15) and (2.16) are taken from [Ref. 3 Tables A-3 and A-6] and correspond to the mean temperatures of each month. The relative humidity of the air ϕ_a is the mean value for each month taken from Table 1.

However, the heat transfer due to evaporation is calculated and shown in Table 5.

TABLE 5. MONTHLY EVAPORATION HEAT LOSSES.

MONTH	Watts	MBtu per month
January	18004.74	45.71
February	19005.16	43.58
March	18383.86	46.67
April	21560.86	52.97
May	25615.48	65.03
June	27083.13	66.54
July	22194.9	56.34
August	23222.93	58.95
September	21529.47	52.89
October	26330.35	66.84
November	19685.38	48.36
December	17834.02	45.27

III. SYSTEM OPERATION

A. SOLAR INSOLATION

The average solar radiation density outside the atmosphere is approximately 1395 W/m^2 [Ref. 6] for a plane normal to the rays of the sun. This solar constant, reaching the earth's surface, reduces because of the atmospheric reflectivity and absorption, which depend on the angle of the incident radiation as well as the local climatic conditions. In general, the average reflectivity is 35% and the absorption 20%. Then the average incident power density is approximately S = (1-0.35)(1-0.2) 1395 W/m^2 = 725 W/m^2 and it occurs at noontime (average maximum value). Designing a solar heating system is of interest to calculate the daily and then the monthly average incident power density, which varies with the time (seasonal variation) as well as the place (geographic position).

1. Geometry of the Incident Solar Radiation

The incident solar power varies due to the daily rotation of the earth and to the varying tilt of its axis with respect to the equatorial plane. This angle varies for a given place in a sinusoidal sense (Figure 5) through the year and gets its maximum value on June 22 (23.5^0) for the northern hemisphere and its minimum one on December 22 (-23.5^0). The above angle is called *declination of the sun* θ_d. Considering a spherical coordinate system (Figure 6) with its origin to the center of the earth, where a_r is the normal vector to the surface of a specific place M, $\pi/2-\theta$ is its latitude and $\phi+\pi/2$ is its hour angle, the incident rays of a flux S impinge on this surface with an angle θ_d with respect to the equatorial plane. In this case, for convenience, it is assumed the sun rays to be in the y - z plane, so noon coincides with $\phi = \pi/2$.

17
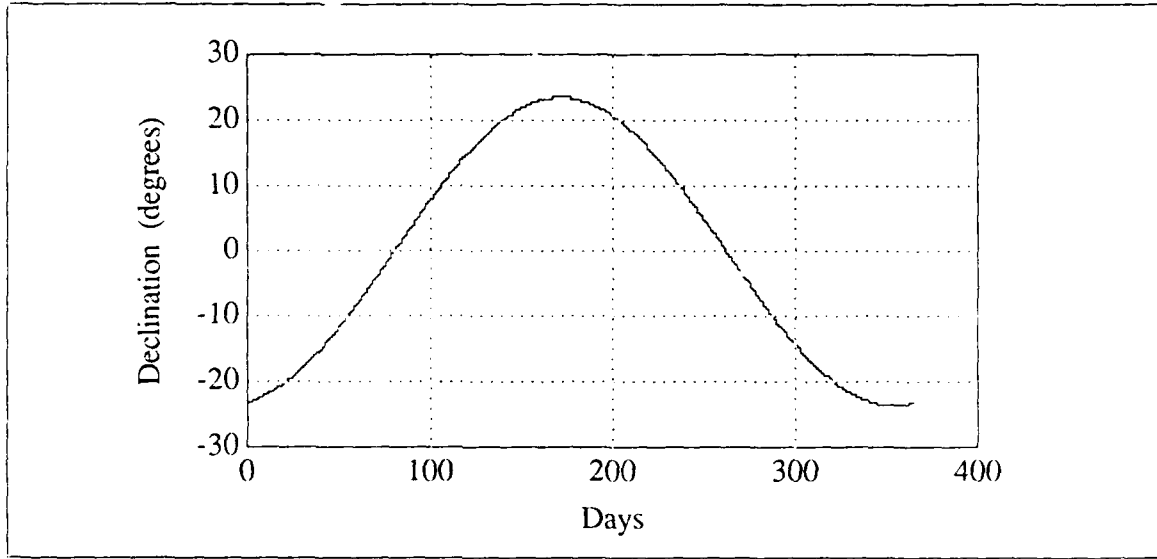
Figure 5. Declination of the sun through the year.

Then the normal incident flux is:

$$S_r = -a_r S \qquad (3.1)$$

Resolving the vectors a_r and S into rectangular components, we have:

$$a_r = a_x \sin\theta \cos\phi + a_y \sin\theta\sin\phi + a_z \cos\theta$$

$$S = -a_y S \cos\theta_d - a_z S \sin\theta_d$$

and substituting in eq. (3.1), we get:

$$S_r = S \cos\theta_d \sin\theta \sin\phi + S \sin\theta_d \cos\theta \qquad (3.2)$$

18
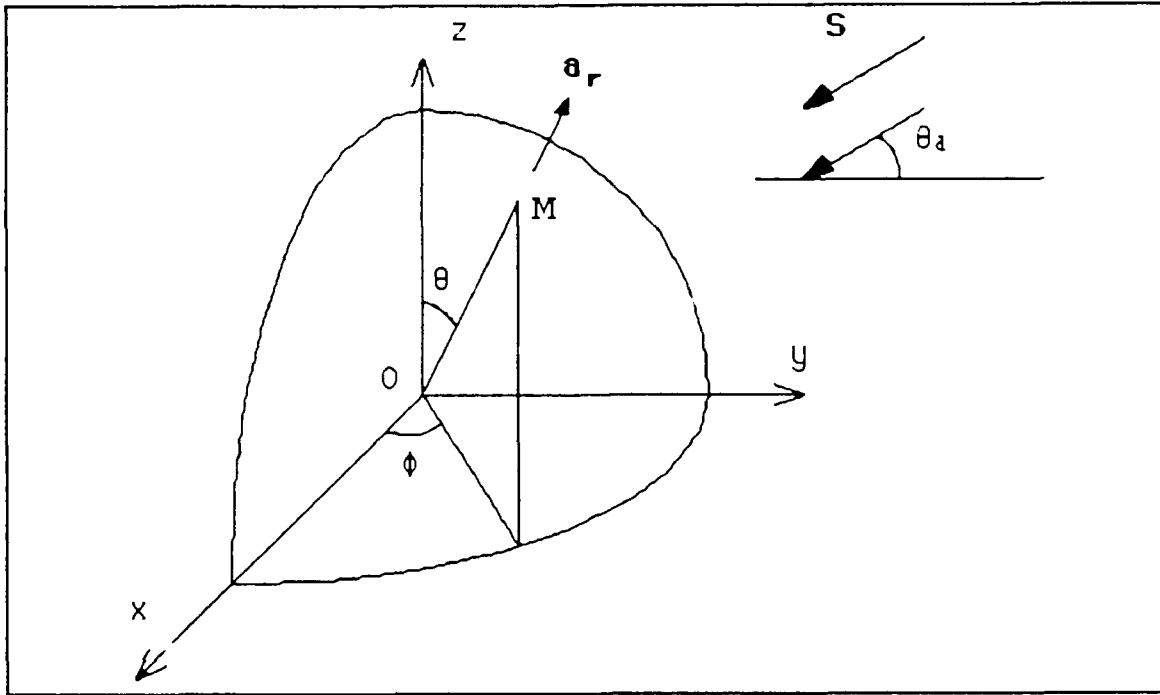
Figure 6. Polar coordinate system for solar radiation.

The above equation gives the incident solar radiation with respect to time (ϕ and θ_d) and position ($\pi/2\text{-}\theta$). To obtain the average daily power density for a particular day we integrate it over the daylight time, that is:

$$S_{rav} = \frac{S}{2\pi} \int_{daylight} (\cos \theta_d \sin \theta \sin \phi + \sin \theta_d \cos \theta) d\phi \qquad (3.3)$$

The corresponding hour angles for the sunrise and sunset are ϕ_m and $(\pi - \phi_m)$, respectively. The sunrise angle ϕ_m corresponds to that ϕ which makes the integrand of eq. (3.3) zero, that is:

19

$$\cos\theta_d \sin\theta \sin\phi_m + \sin\theta_d \cos\theta = 0$$

$$\sin\phi_m = -\frac{\tan\theta_d}{\tan\theta}$$

$$\phi_m = \sin^{-1}\left[-\frac{\tan\theta_d}{\tan\theta}\right]$$
(3.4)

And the eq. (3.3) becomes:

$$
\begin{aligned}
S_{rav} &= \frac{S}{2\pi}\int_{\phi_m}^{\pi-\phi_m}\left(\cos\theta_d \sin\theta \sin\phi + \sin\theta_d \cos\theta\right)d\phi \\
&= \frac{S}{\pi}\int_{\phi_m}^{\pi/2}\left(\cos\theta_d \sin\theta \sin\phi + \sin\theta_d \cos\theta\right)d\phi \\
&= \frac{S}{\pi}\left[\cos\theta_d \sin\theta \cos\phi_m + \sin\theta_d \cos\theta(\pi/2 - \phi_m)\right]
\end{aligned}
$$
(3.5)

In the above eq. (3.4), using the mentioned solar constant (725 W/m^2), and substituting $\theta = 53^0\,25'$ (Monterey latitude $= 36^0\,35'$ N), as θ_d the mean declination of the sun for each month taken from [Ref.10] and as daylight period the mean for each month, the average daily solar insolation is obtained, as shown in Table 6. These results are consistent to the data based on weather statistics and given in [Ref. 7].

2. Optimization of the Solar Collector Tilting

In designing a solar heating system, the solar collector tilting is taken under consideration in order to maximize the received solar power density. The basic concept for a fixed collector is that it must receive solar energy for most of the daylight.

TABLE 6. MEAN DAILY SOLAR INSOLATION (MONTEREY).

	Langley / day	Btu / ft² day	W / m²
January	200	737.4	96.93
February	285	1050.8	138.12
March	430	1585.41	208.39
April	530	1954.11	256.85
May	575	2120	278.66
June	620	2285.94	300.47
July	600	2212.2	290.78
August	540	1991	261.69
September	450	1659.15	218.08
October	350	1290.45	169.62
November	240	884.88	116.31
December	170	627	82.38

Assuming that a_n is normal to the collector surface and α is the angle between the normal and the vertical a_r, then the incident radiation on the collector is:

$$S_n = -a_n S \qquad (3.6)$$

From the geometric relations (Figure 7) substituting in eq. (3.2) the angle θ by $(\theta + \alpha)$, we get:
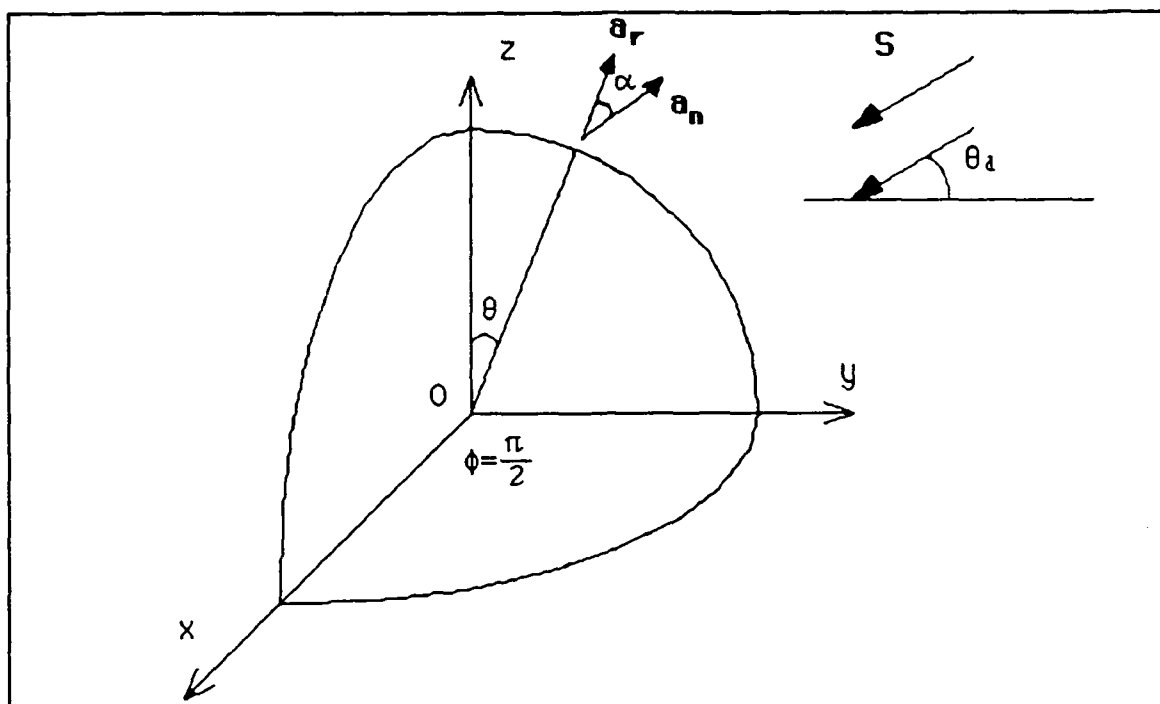
Figure 7. Tilted collector at an angle α with respect to the ground.

$$S_n = S \cos\theta_d \sin(\theta+\alpha) \sin\phi + S \sin\theta_d \cos(\theta+\alpha) \tag{3.7}$$

Integrating eq. (3.7) over the daylight period, the average solar irradiation $S_{n\,av}$ is obtained.

$$
\begin{aligned}
S_{n\,av} &= \frac{S}{2\pi} \int_{daylight} \left[\cos\theta_d \sin(\theta+\alpha)\sin\phi + \sin\theta_d \cos(\theta+\alpha)\right]d\phi \\
&= \frac{S}{2\pi} \int_{\phi_m}^{\pi-\phi_m} \left[\cos\theta_d \sin(\theta+\alpha)\sin\phi + \sin\theta_d \cos(\theta+\alpha)\right]d\phi \\
&= \frac{S}{\pi} \int_{\phi_m}^{\pi/2} \left[\cos\theta_d \sin(\theta+\alpha)\sin\phi + \sin\theta_d \cos(\theta+\alpha)\right]d\phi \\
&= \frac{S}{\pi}\left[\cos\theta_d \sin(\theta+\alpha)\cos\phi_m + \sin\theta_d \cos(\theta+\alpha)(\frac{\pi}{2} - \phi_m)\right] \tag{3.8}
\end{aligned}
$$

22

In order to find the optimal tilting α of the collector for the winter (negative values of sun's declination), we define a variable $S_{n\,total}$ which is the sum of the average solar irradiation $S_{n\,av}$ for each day over the winter time (Sep. 22 through Mar. 22).

Then $S_{n\,total} = \sum_{W\,int\,er} S_{n\,av}(\alpha, \theta_d, \phi_m)$

The total solar irradiation is a function of the angle α and a specific value of it maximizes $S_{n\,total}$. Numerically, we obtain the angle α after a series of runs over a range of feasible angles and record the resulting $S_{n\,total}$. The change of the $S_{n\,total}$ during winter with respect to the tilting angle α, is shown in Figure 8. It can be seen that $S_{n\,total}$ is maximized for $\alpha = 56^0$.
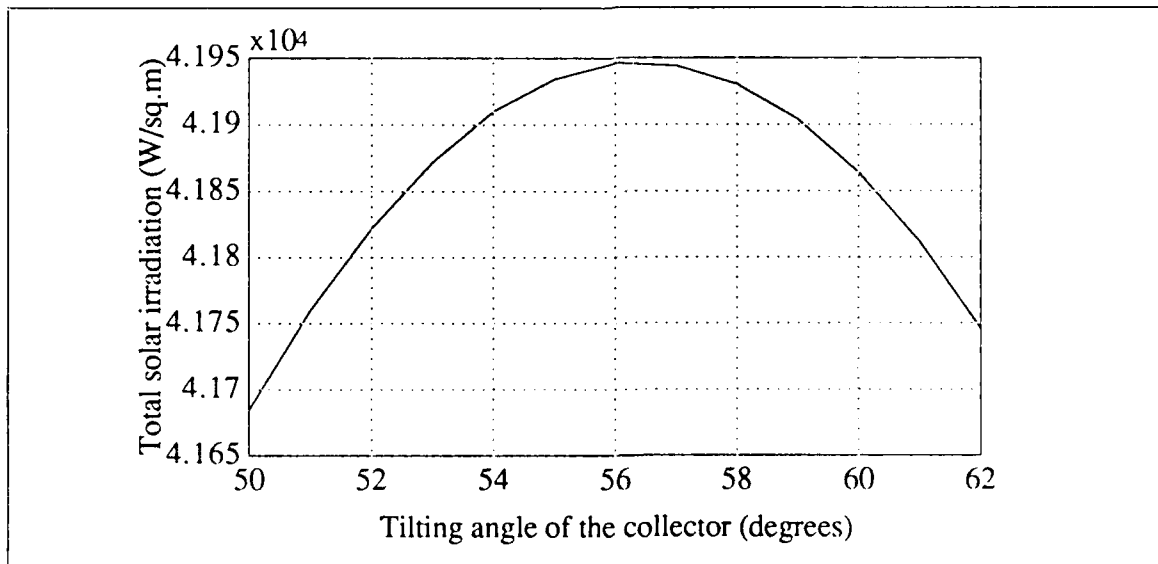
Figure 8. Total solar irradiation received in winter (Sep. 22 through Mar. 22) vs tilting angle of the collector.

23
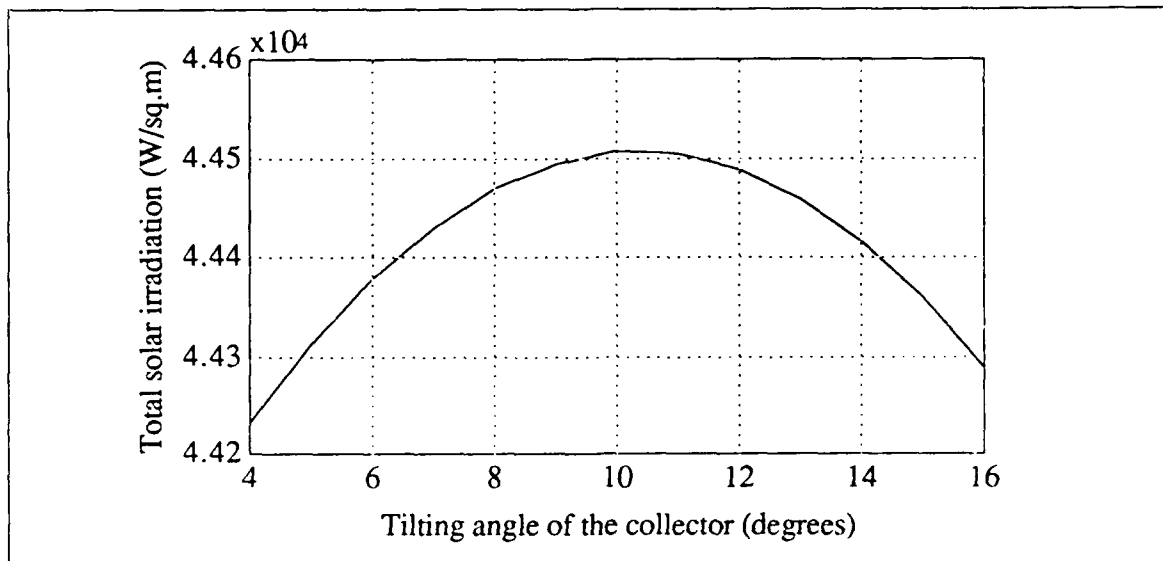
Figure 9. Total solar irradiation received in summer (Mar. 22 through Sep. 22) vs tilting angle of the collector.

If the collector is tilted to operate during the summer (Mar. 22 through Sep.22) and have the maximum efficincy, working similarly we obtain the optimal angle $\alpha = 10^0$ (Figure 9). For a year-round operation, the optimal angle is $\alpha = 33^0$ (Figure 10).
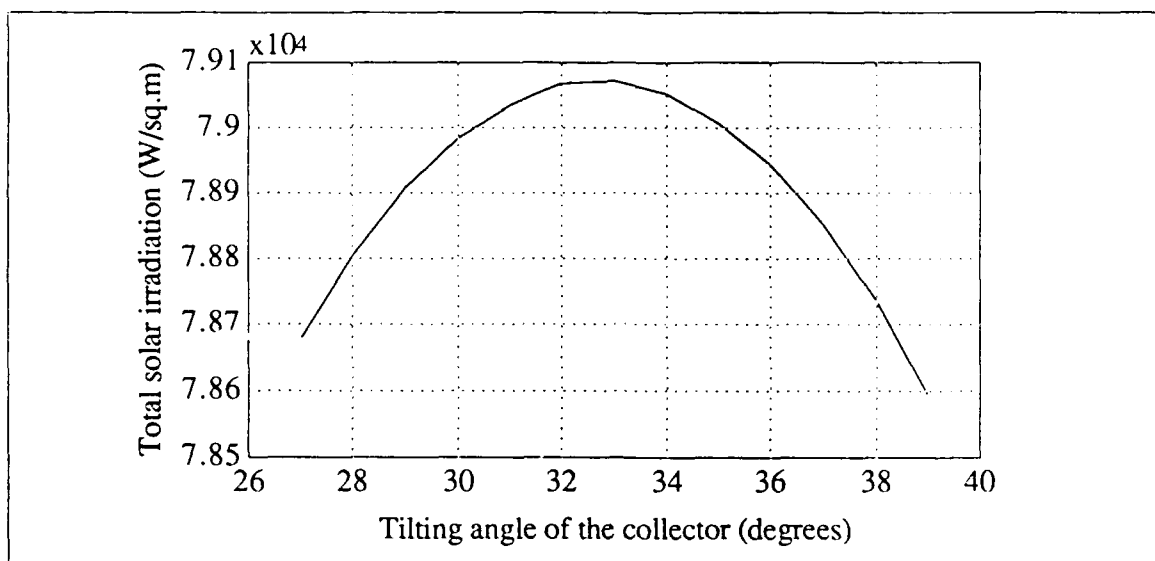
Figure 10. Total solar irradiation received by the collector through the year vs its tilting angle.

B. ENERGY BALANCE

In Chapter II the net heat rate loss Q_L due to heat transfer is calculated for each month (Table 7), taking under consideration the weather conditions, the geometry and the construction of the swimming pool. Solar irradiation q_S has also been calculated (Table 6) for each month and for the Monterey area.

Solar power Q_S is collected by the array and through a heat exchanger delivered to the thermal load (Figure 11). Considering the average efficiency (fraction of the solar irradiation extracted as useful energy) of a collector usually used in this type of heating systems n = 0.7, then the power drawn by the collector is Q_C = n Q_S. Assuming also that the heat exchanger provides to the pool all the thermal energy it receives from the array, and additionally its free surface A_p receives directly a part of the solar power, we model the collector - pool system.
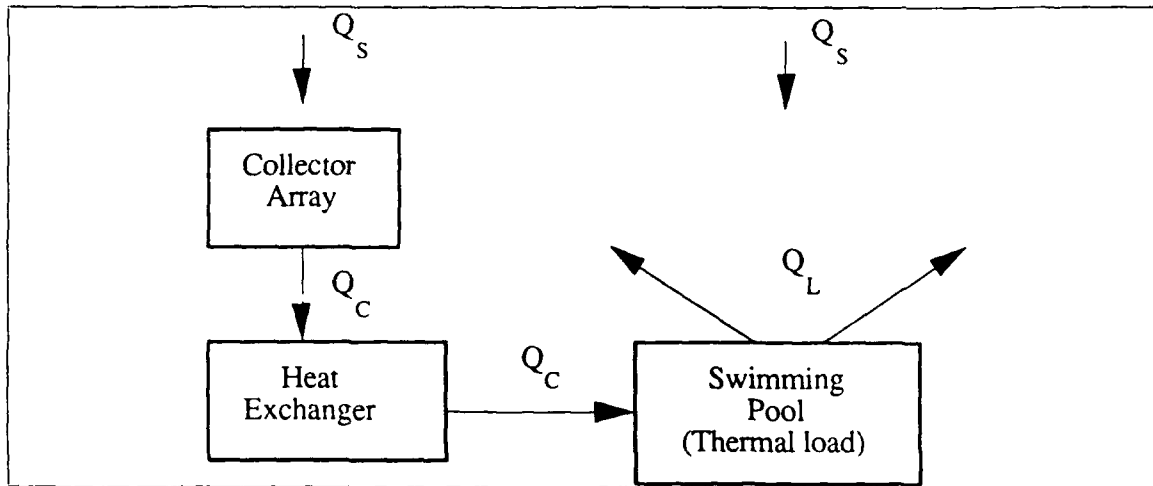
Figure 11. **Block diagram of the energy balance in the collector - pool system.**

$$Q_C + (1\text{-}\rho_S)\, q_S\, A_P = Q_L$$

or

$$n\, Q_S + (1\text{-}\rho_S)\, q_S\, A_P = Q_L \qquad (3.9)$$

where Q_S, Q_C, Q_L are energy rates (Watts), ρ_S is the water reflectivity taken from [Ref. 3], and $(1\text{-}\rho_S)$ is the fraction of the solar power received by the swimming pool surface.

The above relation denotes the energy balance that must exist for the water temperature to be maintained. Eq. (3.9) becomes:

$$n\, A_C q_S + (1\text{-}\rho_S)\, q_S\, A_P = Q_L \qquad (3.10)$$

TABLE 7. TOTAL MONTHLY HEAT LOSS.

MONTH	NET HEAT LOSS (WATTS)	MONTH	NET HEAT LOSS (WATTS)
January	165403	July	161000
February	163018	August	159432
March	162237	September	147236
April	172841	October	162997
May	181948	November	157596
June	176658	December	163493

where q_S, q_L are power densities (W/m^2), $\rho_S = 3$ and A_C is the area of the collector array (m^2) to be calculated. Designing the heating system to operate all year, we are looking for the worst case, where the array will provide energy to balance the greatest loss while the incident solar irradiation will be the least (maximum aperture). This turns to be $A_C = 2183$ m^2 for December. If the heating system is to operate from April through October, then $A_C = 720$ m^2 = 7750 ft^2.

The above calculated areas of the solar collector array, which is to be used in each case, are too large and off the swimming pool site. Up to this point, the design of the heating system was done without taking under consideration the already existing swimming pool cover. Assuming that the pool will be open from 10 a.m. to 6 p.m. and covered the rest of the day, then the net heat loss Q_L will be:

$$Q_L = Q_{cond,w} + 1/3\, Q_{conv,srf} + 2/3\, Q_{cond,cov} + 1/3\, Q_{evap} + 1/3\, Q_{rad,srf} + 2/3\, Q_{rad,cov} \quad (3.11)$$

27

where, $Q_{cond,w}$ is the conduction heat loss through the walls and the bottom of the pool which remains the same after covering (Table 3), $Q_{conv,srf}$ is the convection heat loss from the free water surface which holds for one third of the day (open pool) (Table 4), $Q_{cond,cov}$ is the conduction heat loss through the pool cover which holds for two thirds of the day (covered pool), Q_{evap} is the evaporation loss for open pool only (Table 5), $Q_{rad,srf}$ is the radiation loss through the free water surface (one third of the day), and $Q_{rad,cov}$ is the radiation loss from the pool cover. This cover consists of two polyethylene films and a middle cross linked polyethylene foam layer (Figure 12).

To calculate the conduction heat loss through the cover, we use eq. (2.7) or (2.8) taking under consideration as insulating material the polyethylene foam middle layer only.

$$Q_{conv,cov} = \frac{k_p A}{L_p}\left(T_p - T_a\right)$$

where k_p is the thermal conductivity of the middle layer of the cover, L_p is the thickness of the layer, T_p the temperature of the pool and T_a the average temperature of the air and A the area of the pool. Taking the thermal conductivity coefficient of the polyethylene from the Table A-3 ($k_p = 0.015$ W/mK) and for $L_p = 0.005$ m, $T_p = 300^0$ K, $T_a = 286.33^0$ K (56^0 F for May) and A = 652 m^2, we obtain $Q_{cond,cov} = 46944$ Watt (for May).

For the calculation of $Q_{rad,cov}$, we use eq. (2.14). Then:

$$Q_{rad,cov} = A F \sigma \varepsilon \left(T_p^4 - T_{atm}^4\right) \tag{3.12}$$
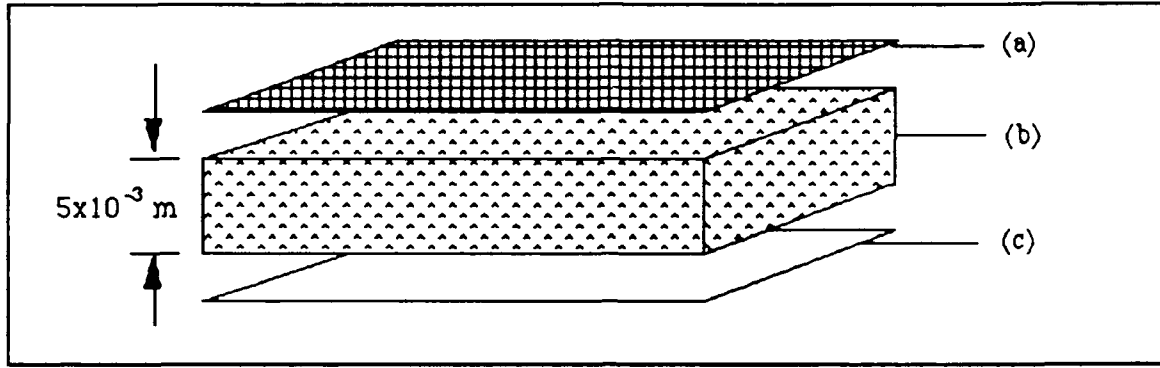
Figure 12. **Cross section of the swimming pool cover:** (a) Polyethylene scrim, (b) cross-linked polyethylene foam, (c) polyethylene film.

where A is the area of the swimming pool surface, F is the view factor and F = 1, σ is the Stefan-Boltzman constant, ε is the emissivity of the outer polyethylene film ($\varepsilon = 0.85$ taken from Ref. 3), $T_p = 300^0$ K, and $T_{atm} = 273^0$ K is the atmosphere temperature. Applying these values in eq. (3.12) we get $Q_{rad,cov} = 79985.34$ Watt.

Substituting in eq. (3.11) all the values of the different losses for a particular month (e.g., for May) we obtain:

$$Q_L = 5242.26 + 0.33 \times 60754.73 + 0.67 \times 46944 + 0.33 \times 25615.48 +$$

$$+ 0.33 \times 90336 + 0.67 \times 79985.34 = 148597.96 \text{ Watt.}$$

Comparing the above result with the total heat loss for May from Table 7 (181948 Watt), we get energy savings 33350 Watt or 18.32%. Working similarly for all the month heat losses, we get an average energy savings of 20%. Then using eq. (3.10), we recalculate the area of the collector array A_c looking again for the worst case (greatest loss -

least solar irradiation), while the pool cover is used to reduce the heat loss of the swimming pool during the night hours. For an all-year operation of the heating system, it is required an array $A_c = 1616$ m^2. If the system operates from April through October, then $A_c = 446$ m^2 = 4800 ft^2.

For a high performance solar heating application, as in this case, a commonly-used collector is the glazed solar collector made of copper plate with copper piping, (Figure 17). A better conductivity of the thermal energy is provided by copper fins roll-formed around the copper tubes. The collector surface is glazed with a high-quality glass which operates as a *heat trap*, reducing radiative and convective losses emitted by the collector. The dimensions of a formal collector panel of this kind are 4'x10'; for the heating system operating in the summer, 120 panels are required and their cost is $1300/panel or $156,000 for the whole collector array including its installation.

C. PUMP AND PIPING

The solar heating system includes two loops of fluid circulation. The collector loop consists of the solar array, the heat exchanger and a pump P_1 for circulating the water through the collector and back to the exchanger (Figure 13). The second loop circulates the water from the exchanger to the filters and then to the pool using a pump P_2. This pump already exists in the old heating system. It has a flow rate of 750 gal/min circulating the pool water roughly three times a day and is driven by standard ac. The other pump P_1 is to be determined with respect to power (h.p.), that is, we have to determine a flow rate (m^3/s) for achieving a good conduction of heat from the collector to the water as it passes through. On the other hand, a large flow rate through the exchanger is a poor practice resulting in excessive pumping and cost. Then P_1 must be adequate for delivering sufficient water flow for good solar collector performance during the summer months where the incident solar irradiation is at its highest (300.47 W/m^2 in June).
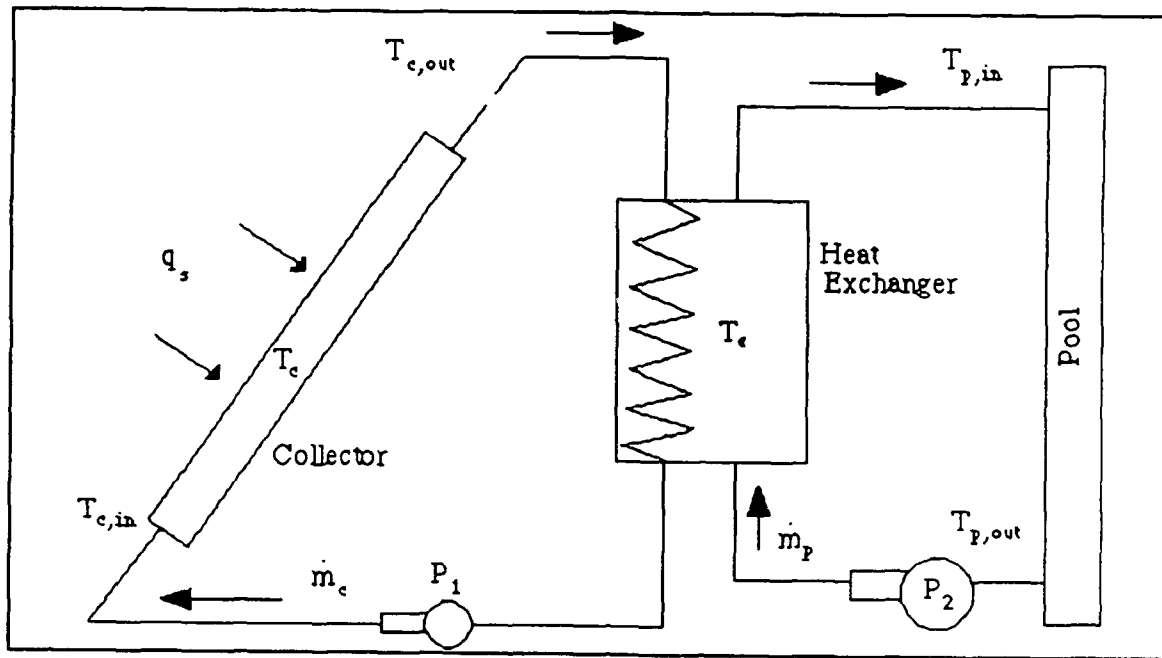
Figure 13. Schematic model of the heating system.

Assuming that all the heat is transferred from the heat collection fluid to the swimming pool water, then the thermal energy in the exchanger is:

$$E_e = (m_c c_c)\Delta T_c - (m_p c_p)\Delta T_p \qquad (3.13)$$

where m_c is the water mass into the collector loop, c_c is the specific heat of the water in an average temperature 330^0K in this loop and $c_c = 4184$ J/kg ^0K, ΔT_c is the decreasing temperature in the exchanger, m_p is the water mass into the swimming pool loop. c_p is the specific heat of the pool water in an average temperature 300^0K in this loop and $c_p = 4180$

J/kg ^{0}K, and ΔT_p is the increasing temperature in the pool. Dividing both parts of eq.(3.13) by time, we get the delivered power by the exchanger to the *load.*

$$Q_e = \left(\dot{m}_c c_c\right)\Delta T_c - \left(\dot{m}_p c_p\right)\Delta T_p \qquad (3.14)$$

where $\dot{m}_c$ and $\dot{m}_p$ are the mass flow rates (Kg/s) provided by P_1 and P_2 respectively. Eq. (3.13) shows that the rate of change of the heat in the exchanger is determined by the rate of heat addition from the collector less the rate of heat removal by the swimming pool (thermal load). Since all the heat is transferred from the collector to the exchanger we have:

$$nA_c q_s = Q_e = \left(\dot{m}_c c_c\right)\Delta T_c - \left(\dot{m}_p c_p\right)\Delta T_p \qquad (3.15)$$

Determining a control strategy where the collector pump P_1 is turned on when $\Delta T_c = T_{c,out} - T_{c,in} = 4^0$K or $\Delta T_p = 2^0$K below the desired average temperature of 300^0K, and taking under consideration that $\dot{m}_p = 750$ gal/min = 47.18 kg/s and $q_s = 300.47$ W/m^2 (for June), we substitute in eq.(3.15) and solving for $\dot{m}_c$,we get a mass flow rate 29.17 Kg/s or 470 gal/min.

Assuming that the piping of the heating system has a 200' length of 5" pipe and that the fittings (90s, tees, 45s, couplers) have an equivalent length of 100' of pipe , then for a flow rate of 500 gal/min, we get from Table A-7 a head loss 3x4.61' = 13.83'.

Then:

Total head loss in pipe and fittings :	13.83'
Height from ground to roof :	10.00'
Approximate friction loss in plumbing :	60.00'
Total head loss .	83.83'

With the operating - system characteristics:

    a. Total head $H = 84$ ft

    b. Pump discharge $U^* = 470$ gal/min

we have to determine the pump P_1 size, revolutions and break horsepower for water circulated at an average temperature 330^0K. In Figure 21 [Ref. 11] using the measured - performance curves for a particular model of a centrifugal water pump with an impeller diameter $D = 35$ in operating in 710 r/min, we get head $H = 187.5$ ft, discharge $U = 19000$ gal/min, and a break horsepower $P = 1000$ bhp.

Given the above data for a model pump and correlating it with our system characteristics we may calculate the break horsepower of P_1 which will be of the same geometric family (centrifugal) and operate at an homologous point (same performance). This correlation can be done by using the similarity rules [Ref. 11], that is, head goes as n^2D^2, discharge as nD^3, and power as $\rho n^3 D^5$, where n is the number of pump revolutions and ρ the water density. The similarity rules are:

$$\frac{H^*}{H} = \left(\frac{n^*}{n}\right)^2 \left(\frac{D^*}{D}\right)^2 \tag{3.16}$$

$$\frac{U^*}{U} = \frac{n^*}{n} \left(\frac{D^*}{D}\right)^3 \tag{3.17}$$

$$\frac{P^*}{P} = \frac{\rho^*}{\rho}\left(\frac{n^*}{n}\right)^3\left(\frac{D^*}{D}\right)^5 \tag{3.18}$$

Applying the values H, D, n, taken from the curves, and H^*, U^* for our system, in the eqations (3.16), (3.17) we get an impeller diameter for P_1 $D^* = 6.73$ in and $n^* = 2472$ r/min. The data of the model pump taken from figure 21 corresponds to a water temperature of 60^0F or 288^0K with density $\rho = 1000$ kg/m^3. In the collector loop (135^0F or 330^0K) the water average density is $\rho^* = 984$ kg/m^3. Substituting ρ^*, n^*, D^*, P, ρ, n, D in eq. (3.18) we obtain $P^* = 11$ bhp or 8.13 kW. This pump costs approximately $3,000.

D. CONTROL UNIT

The controls of any solar heating system can be considered its *brain*. With the aid of sensors, it can determine when heat is available for collection and make the decision when to start and stop the heat collection process. The control systems used in such solar heating systems are called differential temperature controllers. Basically they compare the temperature of the solar panels to that of the *load*, (Figure 14). When the temperature of the panel exceeds that of the load by 4^0C, then a signal is sent by the unit, and the actuating devices are turned on. The collector-to-load differential at which the unit turns on is called turn on delta T. The collector-to-load at which the unit turns off is called turn off delta T. The difference between the turn on and turn off delta T is called temperature hysteresis.

Power is supplied to the controller from 120 Vac household power. The 120 Vac is converted to a lower value dc voltage and is supplied to the collector temperature detection circuitry and collector sensor. The collector temperature detection circuitry receives the
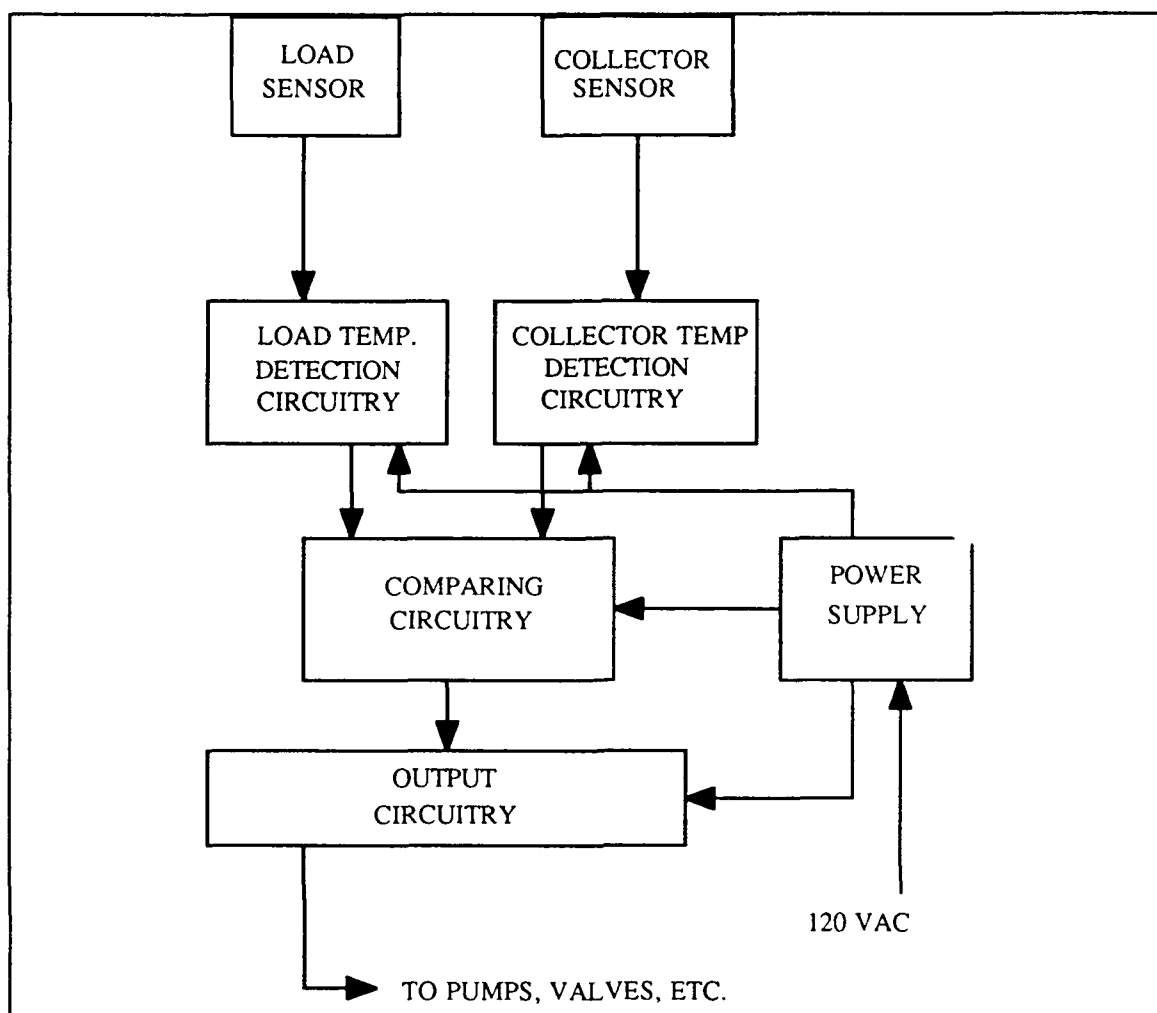
Figure 14. Block diagram of a basic differential temperature controller.

collector temperature as an electrical resistance that changes with temperature. As a result

of this resistance and dc power supplied to the circuit, a voltage is developed within the

detection circuit that is fed to the comparing circuitry. The dc power from the power

supply is also supplied to the load temperature detection circuitry, which operates

identically to the collector temperature detection circuitry. The two voltages fed to the

comparing circuitry are compared constantly. When the comparing circuitry sees that the
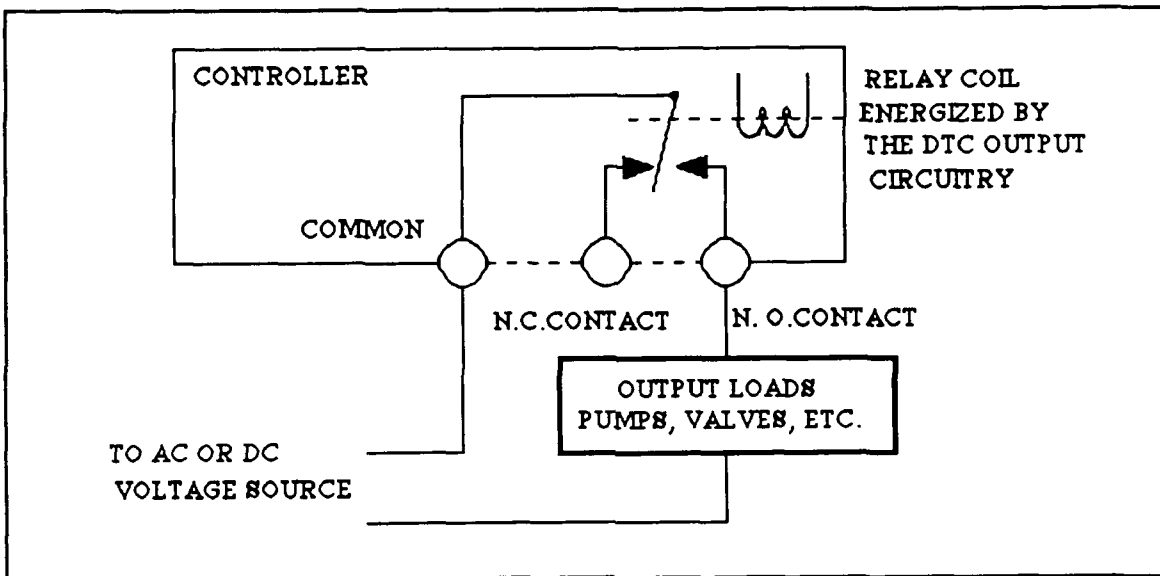
Figure 15. Differential temperature controller output wiring.

collector temperature is greater than that of the load by a set amount, it send̃ a signal to the output circuitry. ˜ ̃e circuitry will energize a relay (Figure 15), whose constants can be sent with whatever power is required to actuate pumps, valves, etc. When the output of the DTC is closure of a set of relay constants, the wiring of the output is as shown in Figure 15.

E. PHOTOVOLTAIC ARRAY DESIGN

The photovoltaic or solar cell converts incoming light into direct current. Figure 16 illustrates a construction of a typical photovoltaic cell which is very similar to a silicon diode. When the front and back contacts are connected to an electrical load, current will flow as a result of the induced voltage and dc electric energy will be generated. The solar cells are assembled into modules which are the smallest units that the consumer will consider. The voltage of a module is determined by the number of solar cells connected in series and usually each cell contributes 0.5 Volts.
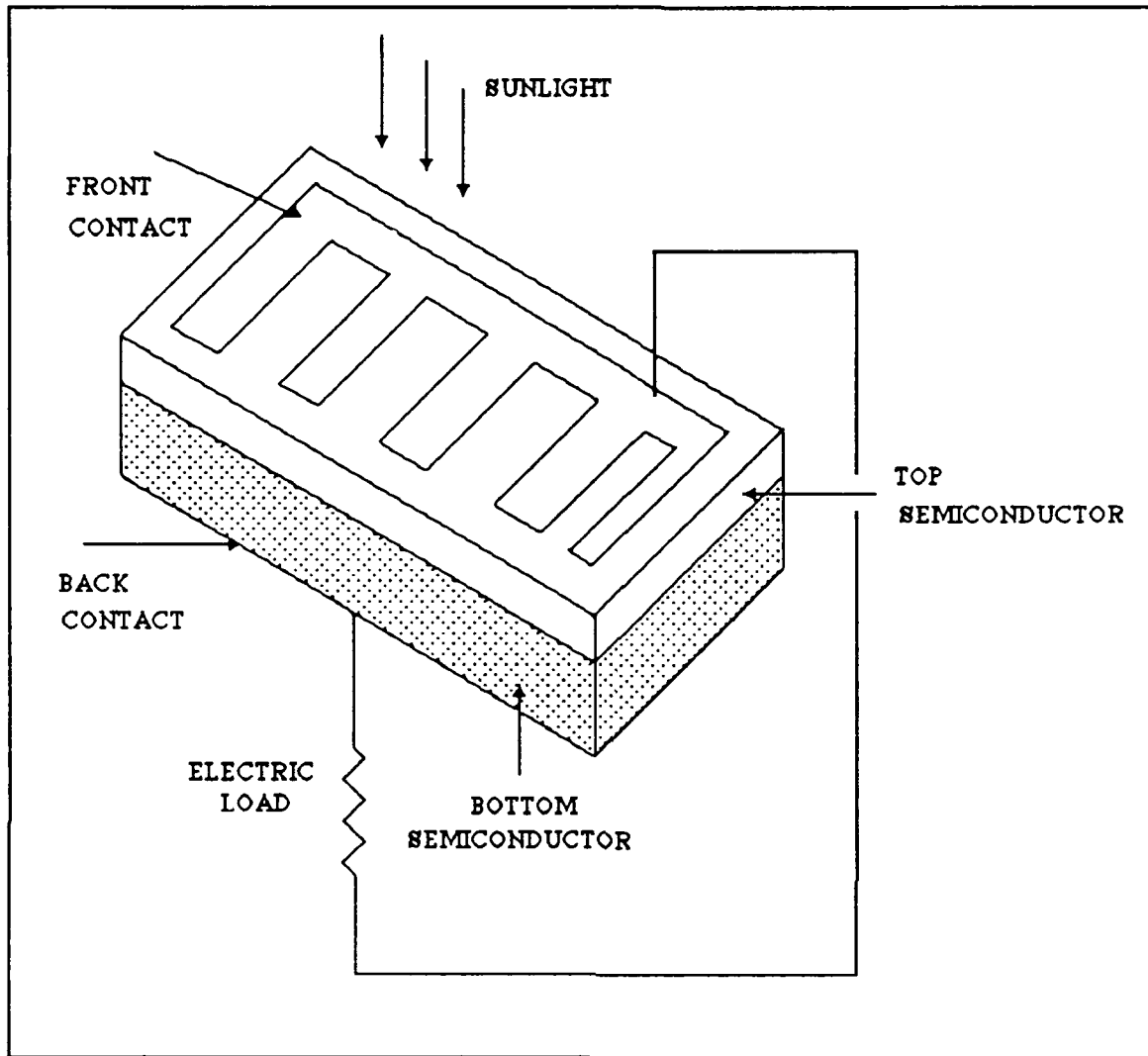
Figure 16. Photovoltaic (solar) cell construction.

The grid - connected photovoltaic system, which is considered as the electric power source for the pump P_1 and the control unit, consists of an array and power conditioner interconnected with ac loads. The power conditiong unit (PCU) controls the operation of the array, starting it up in the morning, shutting it off at night, and maintaining the proper voltage for maximum power extraction. It also converts the variable - voltage dc electrical

output of the array to constant voltage ac electric energy for the load. During a normal operation, the power conditioner controls the array voltage to track automatically maximum power whithin certain limits. When array current exceeds the capability of the power conditioner, such as may occur on a clear day, the unit will increase the array voltage to limit the excess current. When the array power falls below a minimum level the PCU will stop automatically converting energy and shutdown.

The array consists of several series strings of modules which are then paralleled to achieve the desired power level. The series strings are designed to provide a voltage near the center of the power condotioner's input voltage operating range. Since the array configuration depends on PCU properties, the design process begins by choosing the power conditioner and then designing the array. To achieve a desired output the relation between the rating of the power conditioner and the array size is determined by the efficiency of the power conditioner and the average solar insolation. Since the usual PCU efficiency is 74%, then a dc input of about 1.35 kW is needed for each $1kW_{ac}$ and is given by an array of 12 m^2 (130 ft^2) approximately. In order to provide ac electric power 8.5 kW to the pump P_1 and the control unit, it is required an array with output dc power 8.5kW/0.74 = 11.5 kW. For a formal module the manifacturer's specifications under standard operating conditions are the following:

      a. Voltage   12 V

      b. Current   2.5 A

      c. Power   30 W

Then the required area for the array to provide the desired ac power is:

$$S_{array} = 8.5\,kW \times 12\frac{m^2}{kW} = 102\,m^2$$
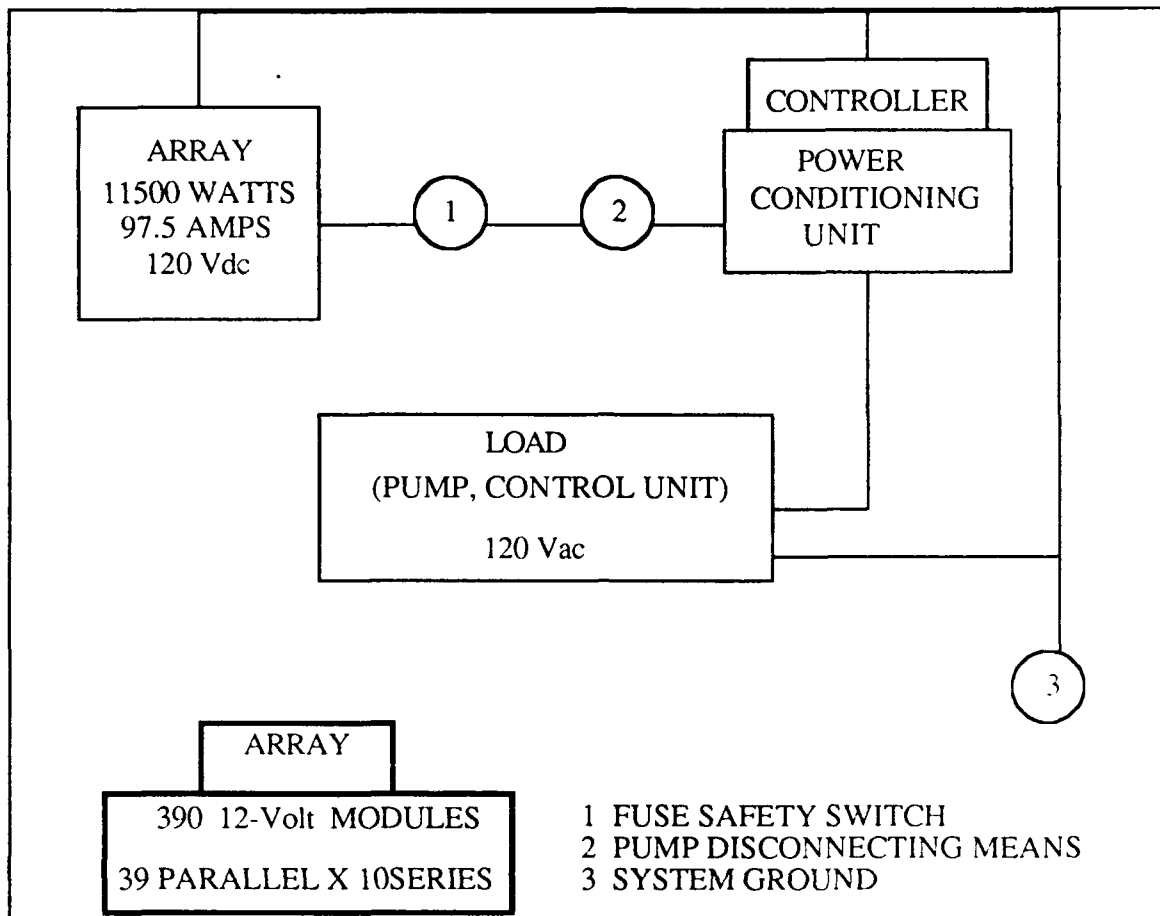
Figure 17. Interconnection of the photovoltaic system with the load.

Finally determining the series / parallel arrangement of modules taking into account the above specifications,we can calculate the number of modules. It is given by:

$$\frac{\text{Array Power}}{\text{Module Power}} = \frac{11500}{30} = 383.3 \cong 384 \text{ modules}$$

while the number of modules per source circuit (series connection) is given by:

$$\frac{\text{Array Voltage}}{\text{Module Voltage}} = \frac{120}{12} = 10 \text{ modules}$$

Then, we determine the number of modules in the array as 390 with 39 modules in parallel connection producing a peak current 97.5 A and 10 in series providing the nominal voltage of 120 Vdc to the pump and the control unit (Figure 17).

Given the specifications of this particular module, the average cost of a panel with a power of 110 Watts is $ 500, that is, the cost of the array is $ 52,000 including the installation.

IV. CONCLUSIONS

Economic consideration of the designed solar heating system is very important to examine and analyze its economic merit and feasibility. The alternative must be compared with the already existing fuel heating system on an equivalent economic basis.

Using records and information from the boiler plant, we calculate the average amount of steam used to heat the pool. From boiler data, 4400 ft^3 of gas produce 4925 lbs of steam, so 1 ft^3 corresponds to 1.12 lbs of steam or 1084 Btu. Also each therm costs $0.90 and the average amount of steam is 20,000 lbs per day. To calculate the cost per day, we use the equation:

$$\text{Cost} = (\text{lbs of steam used}) \times \frac{1\,ft^3\,\text{gas}}{1.12\,\text{lbs steam}} \times \frac{1084\,\text{Btu}}{ft^3\,\text{gas}} \times \frac{1\,\text{therm}}{100000\,\text{Btu}} \times \frac{\$\,0.90}{\text{therm}}$$

which gives a daily cost of $175 or $31,500 for a season of 180 days.

For the designed system the capital cost will be $156,000 + $52,000 + $3,000 = $211,000. Assuming a service life of 10 years with an interest i = 5 % and using the straight - line depreciation plus average interest method, we approximate the true equivalent annual cost. These two variables are obtained from the equations:

$$\text{Straight - line depreciation} = \frac{P - L}{i} \tag{4.1}$$

$$\text{Average interest} = (P - L)\left(\frac{i}{2}\right)\left(\frac{n + 1}{n}\right) + Li \tag{4.2}$$

where,

    P = Capital cost (P = $211,000)

    L = Estimated salvage price (In our case we assume it will be 50 % of the capital cost)

    i = Interest rate

    n = Estimated life time

The annual cost is the depreciation plus the average interest. From eq. (4.1), we get a depreciation of $21,100 and an average interest $8,176. Then the annual cost is $29,276.

However, with our new designed system we are achieving a benefit of roughly $2,200 per year. In this evaluation, the maintenance cost and the personnel payments, which are much lower for a solar heating system, were not taken into consideration. Its efficiency is also dependent on weather conditions, but not on fuel price variations.

APPENDIX A (HEAT TRANSFER TABLES).

TABLE A-1 THERMOPHYSICAL PROPERTIES OF NONMETALLIC MATERIALS.

COMPOSITION	MELTING POINT (K)	ρ (kg/m³)	c_p (J/kg·K)	k (W/m·K)	$\alpha \cdot 10^6$ (m²/s)		PROPERTIES AT VARIOUS TEMPERATURES (K) k (W/m·K) / c_p (J/kg·K)									
							100	200	400	600	800	1000	1200	1500	2000	2500
Graphite fiber epoxy (25% vol) composite	450	1400														
k, heat flow || to fibers				11.1		k	5.7	8.7	13.0							
k, heat flow ⊥ to fibers				0.87		k	0.46	0.68	1.1							
c_p			935			c_p	337	642	1216							
Pyroceram Corning 9606	1623	2600	808	3.98	1.89	k	5.25	4.78	3.64	3.28	3.08	2.96	2.87	2.79		
						c_p		—	908	1038	1122	1197	1264	1498		
Silicon carbide	3100	3160	675	490	230	k		—				87	58	30		
						c_p			880	1050	1135	1195	1243	1310		
Silicon dioxide, crystalline (quartz)	1883	2650														
k, || to c axis				10.4		k	39	16.4	7.6	5.0	4.2					
k, ⊥ to c axis				6.21		k	20.8	9.5	4.70	3.4	3.1					
c_p			745			c_p		—	885	1075	1250					
Silicon dioxide, polycrystalline (fused silica)	1883	2220	745	1.38	0.834	k	0.69	1.14	1.51	1.75	2.17	2.87	4.00			
						c_p		—	905	1040	1105	1155	1195			
Silicon nitride	2173	2400	691	16.0	9.65	k		—	13.9	11.3	9.88	8.76	8.00	7.16	6.20	
						c_p		578	778	937	1063	1155	1226	1306	1377	
Sulfur	392	2070	708	0.206	0.141	k	0.165	0.185								
						c_p	403	606								
Thorium dioxide	3573	9110	235	13	6.1	k			10.2	6.6	4.7	3.68	3.12	2.73	2.5	
						c_p			255	274	285	295	303	315	330	
Titanium dioxide, polycrystalline	2133	4157	710	8.4	2.8	k			7.01	5.02	3.94	3.46	3.28			
						c_p			805	880	910	930	915			

43

TABLE A-1 THERMOPHYSICAL PROPERTIES OF NONMETALLIC MATERIALS (CONTINUED).

COMPOSITION	MELTING POINT (K)	PROPERTIES AT 300K				PROPERTIES AT VARIOUS TEMPERATURES (K) $k\,(W/m\cdot K)/c_p\,(J/kg\cdot K)$									
		ρ (kg/m³)	c_p (J/kg·K)	k (W/m·K)	$\alpha\cdot10^6$ (m²/s)	100	200	400	600	800	1000	1200	1500	2000	2500
Aluminum oxide, sapphire	2323	3970	765	46	15.1	450 / —	82 / —	32.4 / 940	18.9 / 1110	13.0 / 1180	10.5 / 1225				
Aluminum oxide, polycrystalline	2323	3970	765	36.0	11.9	133 / —	55 / —	26.4 / 940	15.8 / 1110	10.4 / 1180	7.85 / 1225	6.55 / —	5.66 / —	6.00 / —	
Beryllium oxide	2725	3000	1030	272	88.0			196 / 1350	111 / 1690	70 / 1865	47 / 1975	33 / 2055	21.5 / 2145	15 / 2750	
Boron	2573	2500	1105	27.6	9.99	190 / —	52.5 / —	18.7 / 1490	11.3 / 1880	8.1 / 2135	6.3 / 2350	5.2 / 2555			
Boron fiber epoxy (30% vol) composite	590	2080													
k, ‖ to fibers				2.29		2.10	2.23	2.28							
k, ⊥ to fibers				0.59		0.37	0.49	0.60							
c_p			1122			364	757	1431							
Carbon Amorphous	1500	1950	—	1.60	—	0.67 / —	1.18 / —	1.89 / —	2.19 / —	2.37 / —	2.53 / —	2.84 / —	3.48 / —		
Diamond, type IIa insulator	—	3500	509	2300		10000 / 21	4000 / 194	1540 / 853							
Graphite, pyrolytic	2273	2210													
k, ‖ to layers				1950		4970	3230	1390	892	667	534	448	357	262	
k, ⊥ to layers				5.70		16.8	9.23	4.09	2.68	2.01	1.60	1.34	1.08	0.81	
c_p			709			136	411	992	1406	1650	1793	1890	1974	2043	

44

TABLE A-2 THERMOPHYSICAL PROPERIES OF MASONRY MATERIALS.

DESCRIPTION/COMPOSITION	TYPICAL PROPERTIES AT 300 K		
	DENSITY, ρ (kg/m^3)	THERMAL CONDUCTIVITY, k (W/m · K)	SPECIFIC HEAT, c_p (J/kg · K)
Building Boards			
Asbestos–cement board	1,920	0.58	—
Gypsum or plaster board	800	0.17	—
Plywood	545	0.12	1,215
Sheathing, regular density	290	0.055	1,300
Acoustic tile	290	0.058	1,340
Hardboard, siding	640	0.094	1,170
Hardboard, high density	1,010	0.15	1,380
Particle board, low density	590	0.078	1,300
Particle board, high density	1,000	0.170	1,300
Woods			
Hardwoods (oak, maple)	720	0.16	1,255
Softwoods (fir, pine)	510	0.12	1,380
Masonry Materials			
Cement mortar	1,860	0.72	780
Brick, common	1,920	0.72	835
Brick, face	2,083	1.3	—
Clay tile, hollow			
1 cell deep, 10 cm thick	—	0.52	—
3 cells deep, 30 cm thick	—	0.69	—
Concrete block, 3 oval cores			
sand/gravel, 20 cm thick	—	1.0	—
cinder aggregate, 20 cm thick	—	0.67	--
Concrete block, rectangular core			
2 cores, 20 cm thick, 16 kg	—	1.1	—
same with filled cores	—	0.60	—
Plastering Materials			
Cement plaster, sand aggregate	1,860	0.72	—
Gypsum plaster, sand aggregate	1,680	0.22	1,085
Gypsum plaster, vermiculite aggregate	720	0.25	—

45

TABLE A-3 THERMOPHYSICAL PROPERIES OF THE AIR.

T (K)	ρ (kg/m^3)	c_p (kJ/kg · K)	$\mu \cdot 10^7$ (N · s/m^2)	$\nu \cdot 10^6$ (m^2/s)	$k \cdot 10^3$ (W/m · K)	$\alpha \cdot 10^6$ (m^2/s)	Pr
Air							
100	3.5562	1.032	71.1	2.00	9.34	2.54	0.786
150	2.3364	1.012	103.4	4.426	13.8	5.84	0.758
200	1.7458	1.007	132.5	7.590	18.1	10.3	0.737
250	1.3947	1.006	159.6	11.44	22.3	15.9	0.720
300	1.1614	1.007	184.6	15.89	26.3	22.5	0.707
350	0.9950	1.009	208.2	20.92	30.0	29.9	0.700
400	0.8711	1.014	230.1	26.41	33.8	38.3	0.690
450	0.7740	1.021	250.7	32.39	37.3	47.2	0.686
500	0.6964	1.030	270.1	38.79	40.7	56.7	0.684
550	0.6329	1.040	288.4	45.57	43.9	66.7	0.683
600	0.5804	1.051	305.8	52.69	46.9	76.9	0.685
650	0.5356	1.063	322.5	60.21	49.7	87.3	0.690
700	0.4975	1.075	338.8	68.10	52.4	98.0	0.695
750	0.4643	1.087	354.6	76.37	54.9	109	0.702
800	0.4354	1.099	369.8	84.93	57.3	120	0.709
850	0.4097	1.110	384.3	93.80	59.6	131	0.716
900	0.3868	1.121	398.1	102.9	62.0	143	0.720
950	0.3666	1.131	411.3	112.2	64.3	155	0.723
1000	0.3482	1.141	424.4	121.9	66.7	168	0.726
1100	0.3166	1.159	449.0	141.8	71.5	195	0.728
1200	0.2902	1.175	473.0	162.9	76.3	224	0.728
1300	0.2679	1.189	496.0	185.1	82	238	0.719
1400	0.2488	1.207	530	213	91	303	0.703
1500	0.2322	1.230	557	240	100	350	0.685
1600	0.2177	1.248	584	268	106	390	0.688
1700	0.2049	1.267	611	298	113	435	0.685
1800	0.1935	1.286	637	329	120	482	0.683
1900	0.1833	1.307	663	362	128	534	0.677
2000	0.1741	1.337	689	396	137	589	0.672
2100	0.1658	1.372	715	431	147	646	0.667
2200	0.1582	1.417	740	468	160	714	0.655
2300	0.1513	1.478	766	506	175	783	0.647
2400	0.1448	1.558	792	547	196	869	0.630
2500	0.1389	1.665	818	589	222	960	0.613
3000	0.1135	2.726	955	841	486	1570	0.536
Ammonia (NH$_3$)							
300	0.6894	2.158	101.5	14.7	24.7	16.6	0.887
320	0.6448	2.170	109	16.9	27.2	19.4	0.870
340	0.6059	2.192	116.5	19.2	29.3	22.1	0.872
360	0.5716	2.221	124	21.7	31.6	24.9	0.872
380	0.5410	2.254	131	24.2	34.0	27.9	0.869
400	0.5136	2.287	138	26.9	37.0	31.5	0.853
420	0.4888	2.322	145	29.7	40.4	35.6	0.833
440	0.4664	2.357	152.5	32.7	43.5	39.6	0.826

TABLE A-4 THERMOPHYSICAL PROPERIES OF THE SATURATED WATER.

TEMPERA-TURE T (K)	PRESSURE P (bars)	SPECIFIC VOLUME (m^3/kg) $v_f \cdot 10^3$	v_g	HEAT OF VAPOR-IZATION h_{fg} (kJ/kg)	SPECIFIC HEAT $(kJ/kg \cdot K)$ $c_{p,f}$	$c_{p,g}$	VISCOSITY $(N \cdot s/m^2)$ $\mu_f \cdot 10^6$	$\mu_g \cdot 10^6$	THERMAL CONDUCTIVITY $(W/m \cdot K)$ $k_f \cdot 10^3$	$k_g \cdot 10^3$	PRANDTL NUMBER Pr_f	Pr_g	SURFACE TENSION $\sigma_f \cdot 10^3$ (N/m)	EXPANSION COEFFICIENT $\beta_f \cdot 10^6$ (K^{-1})	TEMPER-ATURE T (K)
273.15	0.00611	1.000	206.3	2502	4.217	1.854	1750	8.02	569	18.2	12.99	0.815	75.5	-68.05	273.15
275	0.00697	1.000	181.7	2497	4.211	1.855	1652	8.09	574	18.3	12.22	0.817	75.3	-32.74	275
280	0.00990	1.000	130.4	2485	4.198	1.858	1422	8.29	582	18.6	10.26	0.825	74.8	46.04	280
285	0.01387	1.000	99.4	2473	4.189	1.861	1225	8.49	590	18.9	8.81	0.833	74.3	114.1	285
290	0.01917	1.001	69.7	2461	4.184	1.864	1080	8.69	598	19.3	7.56	0.841	73.7	174.0	290
295	0.02617	1.002	51.94	2449	4.181	1.868	959	8.89	606	19.5	6.62	0.849	72.7	227.5	295
300	0.03531	1.003	39.13	2438	4.179	1.872	855	9.09	613	19.6	5.83	0.857	71.7	276.1	300
305	0.04712	1.005	29.74	2426	4.178	1.877	769	9.29	620	20.1	5.20	0.865	70.9	320.6	305
310	0.06221	1.007	22.93	2414	4.178	1.882	695	9.49	628	20.4	4.62	0.873	70.0	361.9	310
315	0.08132	1.009	17.82	2402	4.179	1.888	631	9.69	634	20.7	4.16	0.883	69.2	400.4	315
320	0.1053	1.011	13.98	2390	4.180	1.895	577	9.89	640	21.0	3.77	0.894	68.3	436.7	320
325	0.1351	1.013	11.06	2378	4.182	1.903	528	10.09	645	21.3	3.42	0.901	67.5	471.2	325
330	0.1719	1.016	8.82	2366	4.184	1.911	489	10.29	650	21.7	3.15	0.908	66.6	504.0	330
335	0.2167	1.018	7.09	2354	4.186	1.920	453	10.49	656	22.0	2.88	0.916	65.8	535.5	335
340	0.2713	1.021	5.74	2342	4.188	1.930	420	10.69	660	22.3	2.66	0.925	64.9	566.0	340
345	0.3372	1.024	4.683	2329	4.191	1.941	389	10.89	668	22.6	2.45	0.933	64.1	595.4	345
350	0.4163	1.027	3.846	2317	4.195	1.954	365	11.09	668	23.0	2.29	0.942	63.2	624.2	350
355	0.5100	1.030	3.180	2304	4.199	1.968	343	11.29	671	23.3	2.14	0.951	62.3	652.?	355
360	0.6209	1.034	2.645	2291	4.203	1.983	324	11.49	674	23.7	2.02	0.960	61.4	697.9	360
365	0.7514	1.038	2.212	2278	4.209	1.999	306	11.69	677	24.1	1.91	0.969	60.5	707.1	365
370	0.9040	1.041	1.861	2265	4.214	2.017	289	11.89	679	24.5	1.80	0.978	59.5	728.7	370
373.15	1.0133	1.044	1.679	2257	4.217	2.029	279	12.02	680	24.8	1.76	0.984	58.9	750.1	373.15
375	1.0815	1.045	1.574	2252	4.220	2.036	274	12.09	681	24.9	1.70	0.987	58.6	761	375
380	1.2869	1.049	1.337	2239	4.226	2.057	260	12.29	683	25.4	1.61	0.999	57.6	788	380
385	1.5233	1.053	1.142	2225	4.232	2.080	248	12.49	685	25.8	1.53	1.004	56.6	814	385

TABLE A-5 EMISSIVITY OF NONMETALLIC MATERIALS.

DESCRIPTION / COMPOSITION		TEMPERATURE (K)	EMISSIVITY ε
Silicon carbide	(n)	600	0.87
		1000	0.87
		1500	0.85
Skin	(h)	300	0.95
Snow	(h)	273	0.82–0.90
Soil	(h)	300	0.93–0.96
Rocks	(h)	300	0.88–0.95
Teflon	(h)	300	0.85
		400	0.87
		500	0.92
Vegetation	(h)	300	0.92–0.96
Water	(h)	300	0.96

[a]Adapted from Reference 1.
[b]Adapted from References 1, 9, 20, and 21.

TABLE A-6 THERMAL AND VAPOR DIFFUSIVITY FOR DRY AND SATURATED MOIST AIR.

Temperature F	Degree of Saturation	α ft^2/hr	D ft^2/hr	α/D
50	0	0.770		0.855
			0.901	
	1	0.769		0.854
60	0	0.799		0.854
			0.936	
	1	0.797		0.852
70	0	0.828		0.853
			0.971	
	1	0.826		0.850
80	0	0.858		0.852
			1.007	
	1	0.854		0.848
90	0	0.888		0.851
			1.044	
	1	0.883		0.846
100	0	0.919		0.850
			1.081	
	1	0.911		0.843
110	0	0.949		0.848
			1.119	
	1	0.938		0.838
120	0	0.981		0.848
			1.157	
	1	0.963		0.832
130	0	1.012		0.846
			1.196	
	1	0.985		0.823
140	0	1.044		0.845
			1.235	
	1	1.003		0.812

TABLE A-7 HEAD LOSS AND WATER VELOCITIES INTO PIPES.

Velocity measured in ft./sec., Loss in feet of water head per 100 ft. of pipe.

GALS PER MIN.	½" Vel	Loss	¾" Vel	Loss	1" Vel	Loss	1¼" Vel	Loss	1½" Vel	Loss	2" Vel	Loss	2½" Vel	Loss	3" Vel	Loss	3½" Vel	Loss	4" Vel	Loss
2	2.74	6.72	1.48	1.51																
4	5.48	24.2	2.97	5.45	1.79	1.54	1.00	.39	.73	.177										
6	8.23	51.2	4.45	11.5	2.68	3.34	1.50	.82	1.09	.375	.65	.107								
8	11.0	86.9	5.94	19.6	3.57	5.69	2.00	1.39	1.45	.64	.82	.163	.61	.077						
10	13.7	132.0	7.42	29.6	4.46	8.60	2.50	2.10	1.82	.96	1.09	.276	.76	.115	.485	.039				
12			8.91	41.5	5.36	12.0	3.00	2.94	2.18	1.35	1.30	.387	.91	.161	.572	.055				
15			11.1	62.7	6.7	22.9	3.76	4.45	2.72	2.04	1.63	.555	1.14	.243	.727	.084	.54	.035		
16			13.4	87.9	8.03	25.5	4.50	6.25	3.27	2.86	1.96	.61b	1.36	.340	.873	.116	.65	.056		
20	5" PIPE		14.8	107	8.92	30.9	5.00	7.57	3.63	3.47	2.17	.996	1.51	.414	.97	.140	.72	.068	.56	.037
25					11.2	58.8	6.25	11.4	4.55	5.25	2.71	1.51	1.49	.625	1.21	.212	.90	.103	.69	.055
30	.53	.025			13.4	65.3	7.50	16.0	5.45	7.38	3.26	2.11	2.27	.574	1.45	.297	1.08	.145	.81	.077
35	.62	.044			15.6	86.9	8.75	21.3	6.38	9.72	3.80	2.82	2.65	1.16	1.70	.396	1.26	.192	.93	.103
40	.71	.043			17.9	111	10.0	27.3	7.26	12.5	4.35	3.59	3.63	1.49	1.94	.507	1.44	.246	1.12	.132
45	.795	.054	6" PIPE				11.2	33.9	8.26	15.6	4.89	4.45	3.41	1.56	2.15	.629	1.63	.306	1.25	.164
50	.88	.065	.62	.027			12.5	41.3	9.08	18.9	5.43	5.41	3.79	2.25	2.42	.766	1.83	.372	1.40	.199
55	.973	.078	.676	.032			13.7	49.2	10.00	32.0	5.98	6.44	4.16	2.68	2.67	.912	1.99	.443	1.53	.237
60	1.06	.091	.74	.039			15.0	57.6	10.9	26.5	6.52	7.62	4.54	3.16	2.92	1.07	2.17	.522	1.67	.279
65	1.15	.106	.80	.044			16.1	67.0	11.8	30.7	7.06	8.64	4.92	3.66	3.14	1.25	2.35	.604	1.81	.323
70	1.23	.121	.86	.051			17.5	77.1	12.7	35.3	7.61	10.1	5.30	4.20	3.39	1.43	2.53	.691	1.95	.371
75	1.33	.138	.923	.057			18.6	87.4	13.6	40.1	8.15	11.5	5.65	4.79	3.64	1.62	2.70	.747	2.05	.421
80	1.41	.155	.98	.065			20.0	98.2	14.5	45.2	8.69	12.9	6.05	5.36	3.56	1.83	2.89	.866	2.23	.475
85	1.50	.174	1.04	.072			21.2	110	15.4	50.3	9.03	14.5	6.42	6.02	4.15	2.06	3.05	.992	2.34	.531
90	1.59	.193	1.11	.080			22.5	122	16.3	55.9	9.75	16.1	6.81	6.53	4.33	2.27	3.25	1.10	2.51	.592
95	1.67	.213	1.20	.089					17.2	62.0	10.3	17.6	7.19	7.38	4.57	2.51	3.42	1.21	2.64	.652
100	1.76	.234	1.23	.098					18.2	68.2	10.9	19.6	7.57	8.13	4.85	2.76	3.67	1.34	2.79	.719
110	1.95	.279	1.36	.117					20.0	81.3	12.0	23.4	5.33	9.68	5.33	3.29	3.97	1.60	3.07	.855
120	2.11	.329	1.48	.137	6" PIPE				21.8	95.4	13.0	27.4	9.08	11.4	5.80	3.87	4.33	1.85	3.35	1.00
130	2.3	.351	1.60	.159					23.6	111	14.1	31.8	3.64	13.2	6.30	4.48	4.69	2.18	3.63	1.16
140	2.47	.437	1.72	.182	.95	.047			25.4	127	15.2	36.5	10.6	15.1	6.80	5.12	5.05	2.50	3.91	1.33
150	2.65	.496	1.85	.207	1.05	.054					16.3	41.5	11.3	17.2	7.27	5.87	5.41	2.84	4.19	1.52
160	2.82	.559	1.97	.234	1.12	.059					17.4	46.7	12.1	19.4	7.75	6.58	5.75	3.20	4.47	1.71
170	3.0	.626	2.06	.261	1.19	.067					18.5	52.2	12.9	21.7	8.29	7.37	6.14	3.58	4.75	1.91
180	3.16	.696	2.22	.290	1.26	.074					19.6	58.3	13.6	24.1	8.60	8.18	6.50	3.97	5.02	2.12
190	3.36	.769	2.34	.321	1.33	.082					20.6	64.4	14.4	26.6	9.20	9.05	6.85	4.39	5.30	2.33
200	3.52	.846	2.46	.353	1.41	.090					21.7	70.5	15.1	29.3	9.70	9.96	7.22	4.84	5.58	2.58
220	3.98	1.01	2.71	.421	1.55	.108					23.9	84.1	16.7	34.9	10.6	11.9	7.94	5.75	6.14	3.08
240	4.23	1.18	2.96	.464	1.69	.126					26.1	98.7	18.2	41.0	11.6	13.9	8.66	6.77	6.70	3.62
260	4.58	1.37	3.20	.573	1.83	.147					28.3	115	19.7	47.5	12.6	16.2	9.38	7.85	7.26	4.19
280	4.94	1.57	3.45	.658	1.97	.168							21.2	54.5	13.5	18.6	10.1	9.02	7.82	4.79
300	5.29	1.79	3.69	.747	2.11	.191							22.7	62.0	14.4	21.1	10.8	10.2	8.35	5.45
320	5.64	2.01	3.94	.841	2.24	.215							24.2	69.9	15.5	23.7	11.5	11.5	8.94	6.16
340	5.99	2.26	4.19	.940	2.39	.240							25.8	78.2	16.3	26.6	12.3	12.9	9.50	6.91
360	6.35	2.51	4.43	1.05	2.64	.261							27.2	86.9	17.4	29.5	13.0	14.3	10.0	7.66
380	6.70	2.77	4.68	1.16	2.68	.295							26.8	96.1	18.6	32.6	13.7	15.6	10.6	8.46
400	7.05	3.05	4.93	1.27	2.81	.325							30.3	106	19.4	35.9	14.4	17.4	11.2	9.31
450	7.95	3.79	5.54	1.58	3.16	.404									21.8	44.6	16.2	21.6	12.5	11.6
500	8.83	4.61	6.16	1.92	3.51	.493									23.2	54.1	16.1	26.3	14.0	14.1
550	9.70	5.50	6.77	2.29	3.86	.557									26.5	64.9	19.9	31.4	15.3	16.5
600	10.6	6.44	7.39	2.69	4.22	.666									29.1	76.1	21.7	36.9	16.7	19.7
650	11.5	7.47	8.00	3.12	4.57	.799											23.5	42.5	18.1	22.9
700	12.3	8.60	8.63	3.58	4.92	.916											25.3	48.9	19.5	26.2
750	13.2	9.77	9.24	4.07	5.27	1.04											27.1	55.9	20.9	29.8
800	14.1	11.0	9.85	4.58	5.62	1.17											28.9	61.6	22.3	33.6
850	15.0	12.3	10.5	5.12	5.97	1.31											30.7	70.5	23.7	37.6
900	15.9	13.7	11.1	5.69	6.32	1.46													25.1	41.8
950	16.7	15.1	11.7	6.29	6.67	1.61														
1000	17.6	16.6	12.3	6.91	7.03	1.77														
1100	19.4	19.8	13.5	8.27	7.83	2.11														
1200	21.1	23.3	14.8	9.73	8.43	2.48														
1300					9.13	2.67														
1400					9.53	3.30														
1500					10.5	3.75														
1600					11.2	4.23														
1800					12.6	5.26														
2000					14.1	6.3y														
2200					15.5	7.80														

*Data shown is calculated from Williams and Hazen formula

$$H = \frac{3.023 \cdot V^{1.852}}{C^{1.85} \cdot D^{1.167}}$$

using C = 150. For water at 60°F. Where H = head loss, V = fluid velocity ft./sec., D = diameter of pipe, ft. C = coefficient representing roughness of pipe interior surface.
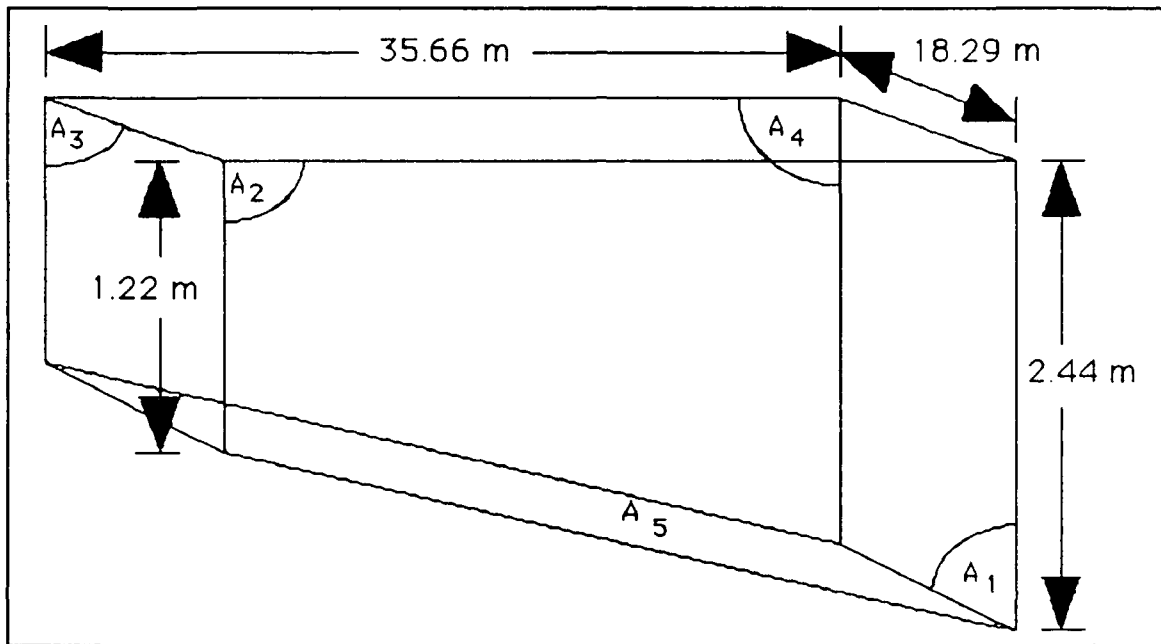
50

Figure 18.   Three-dimension plan of the Naval Postgraduate School swimming pool.
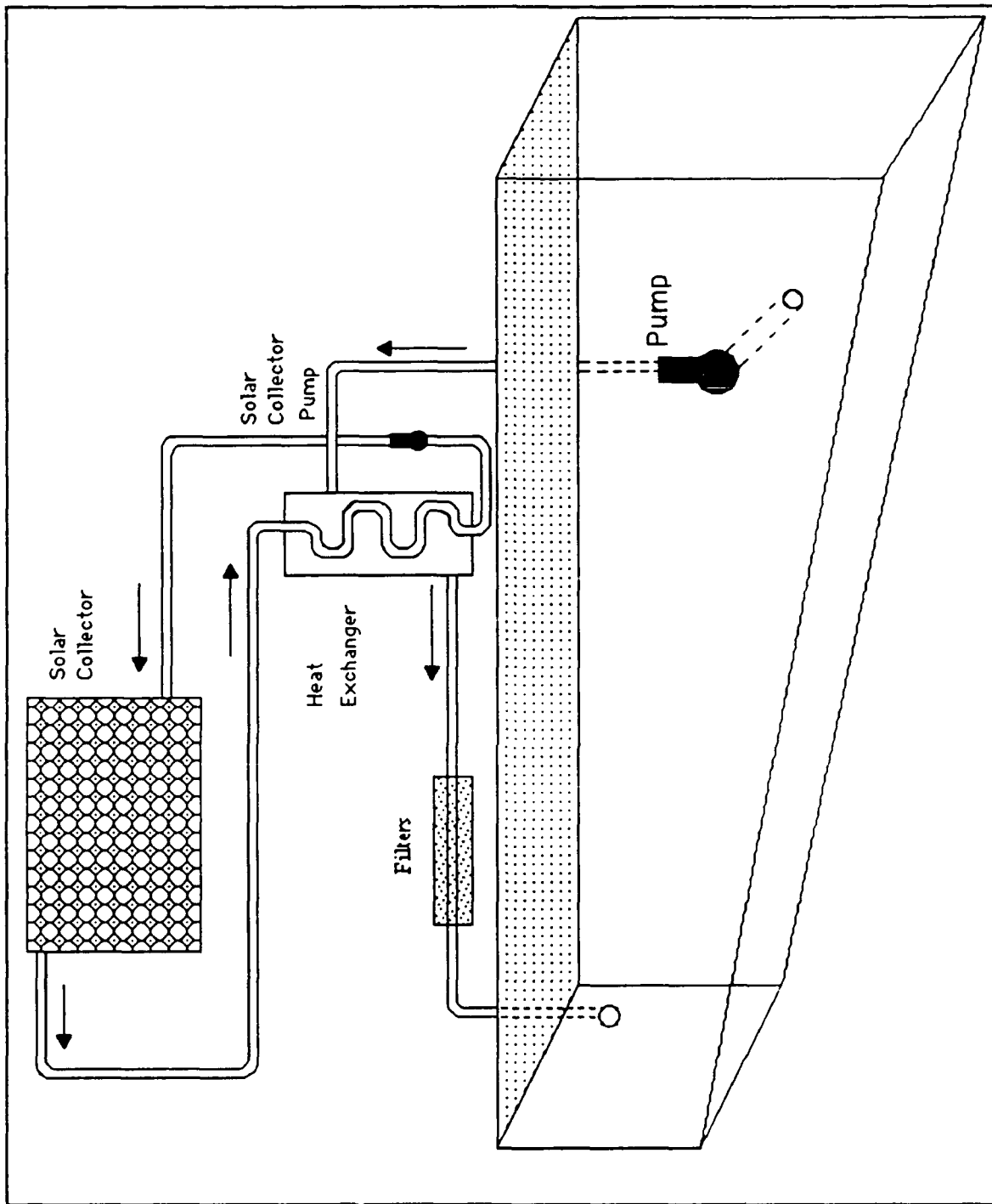
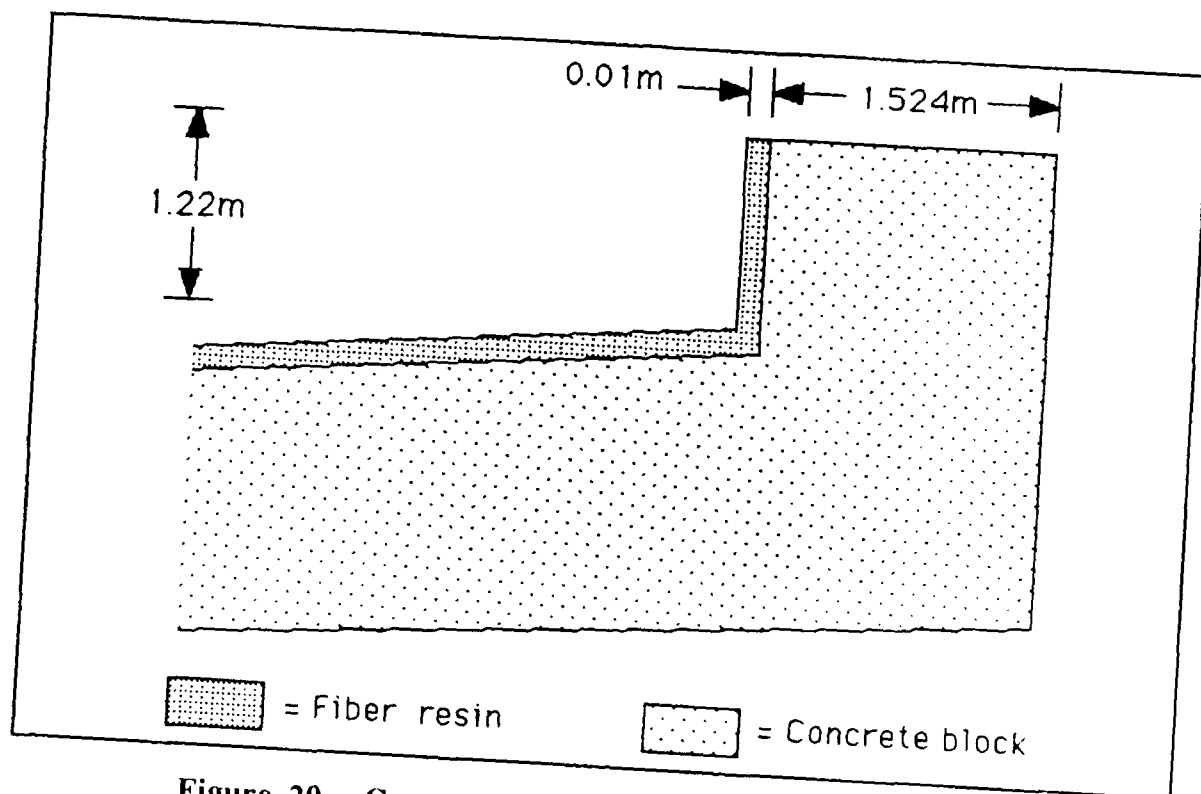Figure 19. Heating system of the swimming pool.

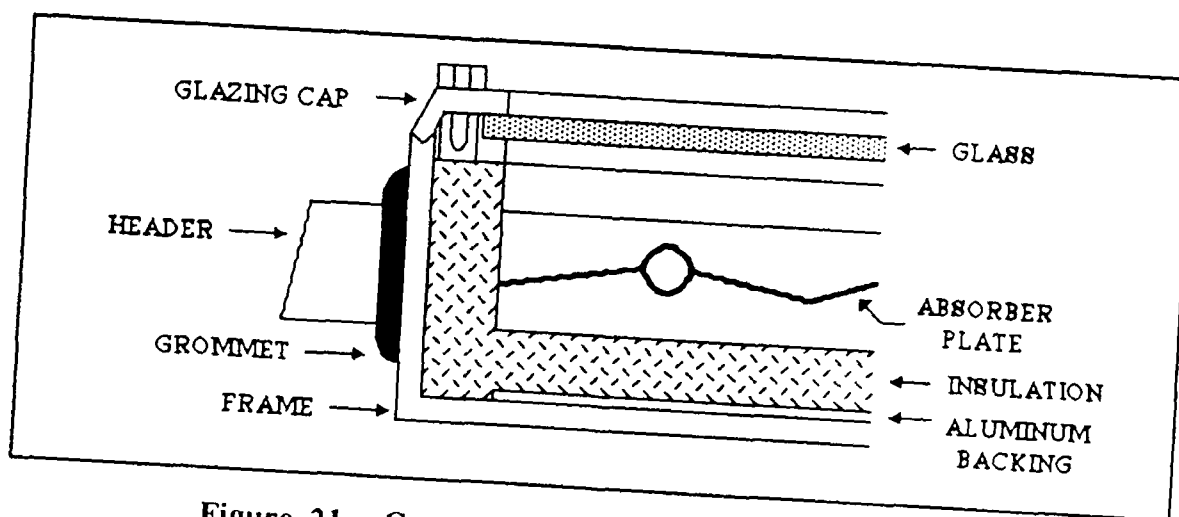**Figure 20.** Cross section of the swimming pool walls.

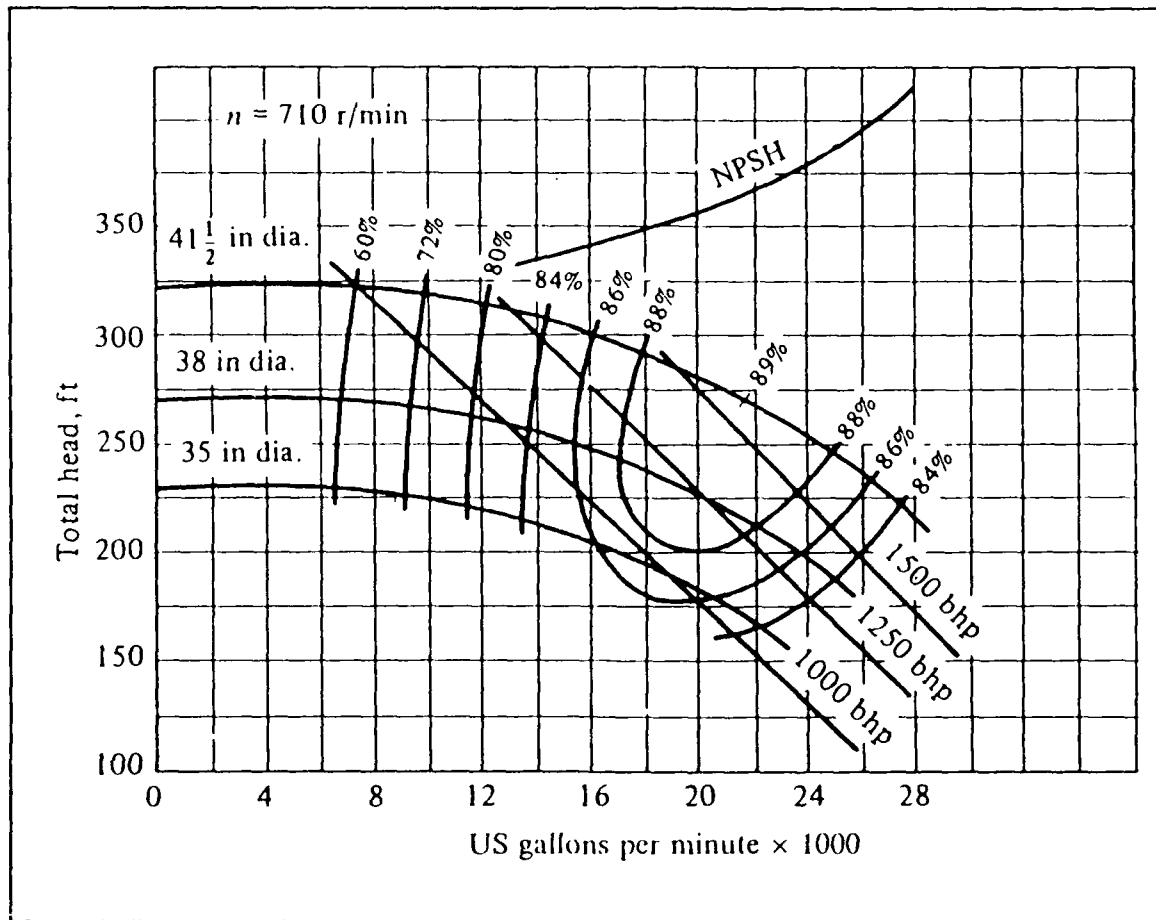**Figure 21.** Cross section of the glazed solar panel.

53

Figure 22.   Measured performance curves for three models of a centrifugal pump.

APPENDIX C (OPTIMIZATION).

```
echo on

clc

% It plots the total solar irradiation (W/sq.m) vs tilting angle of the

%collector for the winter time.

x=[50,51,52,53,54,55,56,57,58,59,60,61,62];

y=[41685,41760,41823,41873,41910,41934,41946,41944,41930,41904,41864,41812,4
1747];

plot(x,y);grid;

xlabel('Tilting angle of the collector (degrees)');

ylabel('Total solar irradiation (W/sq.m)');
```

```
echo on

clc

% It plots the total solar irradiation (W/sq.m) vs tilting angle of the

% collector for the summer time.

x=[4,5,6,7,8,9,10,11,12,13,14,15,16];

y=[44234,44313,44378,44431,44469,44494,44506,44504,44488,44459,44416,44360,4
4290];

plot(x,y);grid;

xlabel('Tilting angle of the collector (degrees)');

ylabel('Total solar irradiation (W/sq.m)');
```

```
echo on

clc

% It plots the total solar irradiation (W/sq.m) vs tilting angle of the % %collector for all

over the year.

x=[27,28,29,30,31,32,33,34,35,36,37,38,39];

y=[78680,78806,78907,78985,79038,79067,79072,79053,79010,78943,78852,78737,7

8598];

plot(x,y);grid;

ylabel('Total solar irradiation (W/sq.m)');

xlabel('Tilting angle of the collector (degrees)');

echo on

clc

a=0.06981317007;

theta=0.9322967;

Snav=0;

Sntotal=0;

S=725;

for x=80:264;

   thetad=0.41015237422*sin(2*pi*(x-80)./365);

   phi=asin(-tan(thetad)./tan(theta));

      Snav=(S/pi)*(cos(thetad)*sin(theta+a)*cos(phi)+sin(thetad)*cos(theta+a)*((pi/2)-

phi));

Sntotal=Sntotal+Snav;

end

Sntotal
```

REFERENCES

1. D. E. KIRK, *Optimal Control Theory*, p. 53-95, Prendice-Hall, 1970.

2. F. L. LEWIS, *Optimal Control*, John Wiley &Sons, p. 293-318, 1986.

3. F. P. INCOPERA and D. P. DE WITT, *Introduction to Heat Transfer*, John Wiley & Sons, 1990.

4. W. C. REYNOLDS and H. C. PERKINS, *Engineering Thermodynamics*, p. 614-615, 1977.

5. J. L. THRELKELD, *Thermal Environmental Engineering*, p. 215-233, Prentice-Hall, Co, 1970.

6. J. H. KRENZ, *Energy Conversion and Utilization*, Allyn &Bacon, Inc. 1976.

7. I. BENNETT, *Monthly Maps of Mean Daily Insolation for the United States*,Solar Energy, Vol. 9, March 1963.

8. J. KLIMA, *Differential Controls for Domestic Hot Water Systems*, 1981.

9. J. R. HOWELL, *Solar-Thermal Energy Systems Analysis and Design*, McGraw-Hill,Inc,1982.

10. *Almanac for Computers*, p.B4-B5,US Naval Observatory, 1980.

11. FRANK M. WHITE, *Fluid Mechanics*, McGraw Hill, Inc, 1986.

INITIAL DISTRIBUTION LIST

		No. Copies
1.	Defense Technical Information Center Cameron Station Alexandria, VA 22314-6145	2
2.	Library, Code 52 Naval Postgraduate School Monterey, CA 93943-5100	2
3.	Chairman, Code EC Naval Postgraduate School Department of Electrical and Computer Engineering Monterey, CA 93943-5000	1
4.	Professor Harold A. Titus, Code EC/Ts Department of Electrical and Computer Engineering Naval Postgraduate School Monterey, CA 93943-5000	4
5.	Professor Sherif Michael, Code EC/Mi Department of Electrical and Computer Engineering Naval Postgraduate School Monterey, CA 93943-5000	1
6.	Dimitrios Vourazelis Hatzigeorgiou 1 Eleusis 19200 Greece	3
7.	Dimitrios Dariotis Kifisias 38 Ambelokipoi 11526 Athens, Greece	1
8.	Embassy of Greece Naval Attache 2228 Massachusetts Ave., N.W. Washington, D.C. 20008	1